SIAM J. FINANCIAL MATH.
Vol. 10, No. 1, pp. 89–129

The Randomized Heston Model*

Antoine Jacquier† and Fangwei Shi†

Abstract. We propose a randomized version of the Heston model—a widely used stochastic volatility model in mathematical finance—assuming that the starting point of the variance process is a random variable. In such a system, we study the small- and large-time behaviors of the implied volatility and show that the proposed randomization generates a short-maturity smile much steeper ("with explosion") than in the standard Heston model, thereby palliating the deficiency of classical stochastic volatility models in short time. We precisely quantify the speed of explosion of the smile for short maturities in terms of the right tail of the initial distribution, and in particular show that an explosion rate of t^γ ($\gamma \in [0, 1/2]$) for the squared implied volatility—as observed on market data—can be obtained by a suitable choice of randomization. The proofs are based on large deviations techniques and the theory of regular variations.

Key words. stochastic volatility, large deviations, Heston, implied volatility, asymptotic expansion

AMS subject classifications. 60F10, 91G20, 91B70

DOI. 10.1137/18M1166420

1. Introduction.

Implied volatility is one of the most important observed data in financial markets and represents the price of European options, reflecting market participants' views. Over the past two decades, a number of (stochastic) models have been proposed in order to understand its dynamics and reproduce its features. In recent years, a lot of research has been devoted to understanding the asymptotic behavior (large strikes [8, 9, 13], small/large maturities [24, 25, 26, 49]) of the implied volatility in a large class of models in extreme cases; these results not only provide closed-form expressions (usually unavailable) for the implied volatility, but also shed light on the role of each model parameter and, ultimately, on the efficiency of each model.

Continuous stochastic volatility models driven by Brownian motion effectively fit the volatility smile (at least for indices); the widely used Heston model, for example, is able to fit the volatility surface for almost all maturities [33, section 3], but becomes inaccurate for small maturities. The fundamental reason is that small-maturity data is much steeper (for small strikes)—the so-called short-time explosion—than the smile generated by these stochastic volatility models (a detailed account of this phenomenon can be found in the volatility bible [33, Chapters 3 and 5]). To palliate this issue, Gatheral (among others) comments

*Received by the editors January 22, 2018; accepted for publication (in revised form) November 21, 2018; published electronically February 12, 2019.

http://www.siam.org/journals/sifin/10-1/M116642.html

Funding: The work of the first author was supported by EPSRC First Grant EP/M008436/1. The work of the second author was funded by a mini-DTC scholarship from the Department of Mathematics, Imperial College London.

†Department of Mathematics, Imperial College London, London SW7 2AZ, UK (a.jacquier@imperial.ac.uk, fangwei.shi12@imperial.ac.uk).

that jumps should be added in the stock dynamics; the literature on the influence of the jumps is vast, and we only mention here the clear review by Tankov [49] in the case of exponential Lévy models, where the short-time implied volatility explodes at a rate of $|t \log t|$ for small t. To observe nontrivial convergence (or divergence), Mijatović and Tankov [47] introduced maturity-dependent strikes and studied the behavior of the smile in this regime.

As an alternative to jumps, a portion of the mathematical finance community has recently been advocating the use of fractional Brownian motion (with Hurst parameter $H < 1/2$) as driver of the volatility process. Alòs, León, and Vives [2] first showed that such a model is indeed capable of generating steep volatility smiles for small maturities (see also the recent work by Fukasawa [31]), and Gatheral, Jaisson, and Rosenbaum [34] recently showed that financial data exhibits strong evidence that volatility is "rough" (an estimate for SPX volatility actually gives $H \approx 0.14$). Guennoun et al. [36] investigated a fractional version of the Heston model and proved that as t tends to zero, the squared implied volatility explodes at a rate of $t^{H-1/2}$. This is currently a very active research area, and the reader is invited to consult [7, 21, 22, 23, 28] for further developments. This is, however, not the end of the story—yet—as computational costs for simulation are a serious concern in fractional models.

We propose here a new class of models, namely standard stochastic volatility models (driven by standard Brownian motion) where the initial value of the variance is randomized, and we focus our attention on the Heston version. The motivation for this approach originates from the analysis of forward-start smiles by Jacquier and Roome [39, 40], who proved that the forward implied volatility explodes at a rate of $t^{1/4}$ as t tends to zero. A simple version of our current study is the "CEV-randomized Black–Scholes model" introduced in [41], where the Black–Scholes volatility is randomized according to the distribution generated from an independent CEV process; in this work, the authors proved that this simplified model generates the desired explosion of the smile. The Black–Scholes randomized setting where the volatility has a discrete distribution corresponds to the lognormal mixture dynamics studied in [11, 12]. We push the analysis further here; our intuition behind this new type of model is that the starting point of the volatility process is actually not observed accurately, but only to some degree of uncertainty. Traders, for example, might take it as the smallest (maturity-wise) observed at-the-money implied volatility. Our initial randomization aims at capturing this uncertainty. This approach was recently taken by Mechkov [46], considering the ergodic distribution of the CIR process as starting distribution, who argues that randomizing the starting point captures potential hidden variables. One could also potentially look at this from the point of view of uncertain models, and we refer the reader to [29] for an interesting related study. The main result of our paper is to provide a precise link between the explosion rate of the implied volatility smile for short maturities and the choice of the (right tail of the) initial distribution of the variance process. The following table (a more complete version with more examples can be found in Table 1) gives an idea of the range of explosion rates that can be achieved through our procedure; for each suggested distribution of the initial variance, we indicate the asymptotic behavior (up to a constant multiplier) of the (square of the) out-of-the-money implied volatility smile (in the first row, the function f will be determined precisely later, but the absence of time dependence is synonymous with absence of explosion).

Name	Behaviors of $\sigma_t^2(x)$ $(x \neq 0)$	Reference
Uniform	$f(x)$	Equation 4.3
Exponential(λ)	$\lvert x\rvert t^{-1/2}$	Theorem 4.11
χ-squared	$\lvert x\rvert t^{-1/2}$	Theorem 4.11
Rayleigh	$x^{2/3}t^{-1/3}$	Theorem 4.5
Weibull ($k > 1$)	$(x^2/t)^{1/(1+k)}$	Theorem 4.5

The rest of the paper is structured as follows: We introduce the randomized Heston model in section 2 and discuss its main properties. Section 3 is a numerical appetizer to give a taste of the quality of such a randomization. Section 4 is the main part of the paper, in which we prove large deviations principles for the log-price process and translate them into short- and large-time behaviors of the implied volatility. In particular, we prove the claimed relation between the explosion rate of the small-time smile and the tail behavior of the initial distribution. The small-time limit of the at-the-money implied volatility is, as usual in this literature, treated separately in section 4.5. Section 5 includes a dynamic pricing framework: based on the distribution at time zero and the evolution of the variance process, we discuss how to reprice (or hedge) the option during the life of the contract. Finally, section 6 presents numerical examples and examples of common initial distributions. The appendices gather some reminders on large deviations and regular variations, as well as proofs of the main theorems.

Notation. Throughout this paper, we denote by $\sigma_t(x)$ the implied volatility of a European Call or Put option with strike e^x and time to maturity t. For a set $\mathcal{S}$ in a given topological space we denote by $\mathcal{S}^o$ and $\overline{\mathcal{S}}$ its interior and closure. Let $\mathbb{R}_+ := [0,\infty)$, $\mathbb{R}_+^* := (0,\infty)$, and $\mathbb{R}^* := \mathbb{R} \setminus \{0\}$. For two functions f and g, and $x_0 \in \mathbb{R}$, we write $f \sim g$ as x tends to x_0 if $\lim_{x\to x_0} f(x)/g(x) = 1$. If a function f is defined and locally bounded on $[x_0,\infty)$, and $\lim_{x\uparrow\infty} f(x) = \infty$, define $f^{\leftarrow}(x) := \inf\{y \geq [x_0,\infty) : f(y) > x\}$ as its generalized inverse. Also define the sign function as $\mathrm{sgn}(u) := \mathbf{1}_{\{u\geq 0\}} - \mathbf{1}_{\{u<0\}}$. Finally, for a sequence $(Z_t)_{t\geq 0}$ satisfying a large deviations principle as t tends to zero with speed $g(t)$ and good rate function Λ_Z^* (Appendix B.1) we use the notation $Z \sim \mathrm{LDP}_0(g(t),\Lambda_Z^*)$. If the large deviations principle holds as t tends to infinity, we denote it by $\mathrm{LDP}_\infty(\cdots)$.

2. Model and main properties.

On a filtered probability space $(\Omega,\mathcal{F},(\mathcal{F}_t)_{t\geq 0},\mathbb{P})$ supporting two independent Brownian motions $W^{(1)}$ and $W^{(2)}$, we consider a market with no interest rates, and propose the following dynamics for the log-price process:

$$\begin{aligned} \mathrm{d}X_t &= -\frac{1}{2}V_t\mathrm{d}t + \sqrt{V_t}\left(\rho\,\mathrm{d}W_t^{(1)} + \overline{\rho}\,\mathrm{d}W_t^{(2)}\right), \quad X_0 = 0, \\ \mathrm{d}V_t &= \kappa(\theta - V_t)\mathrm{d}t + \xi\sqrt{V_t}\mathrm{d}W_t^{(1)}, \qquad\qquad V_0 \overset{(\mathrm{Law})}{=} \mathcal{V}, \end{aligned} \tag{2.1}$$

where $\rho \in [-1,1]$, $\overline{\rho} := \sqrt{1-\rho^2}$, and κ,θ,ξ are strictly positive real numbers. Here $\mathcal{V}$ is a continuous random variable, independent of the filtration $(\mathcal{F}_t)_{t\geq 0}$, for which the interior of the support is of the form $(\mathfrak{v}_-,\mathfrak{v}_+)$ for some $0 \leq \mathfrak{v}_- \leq \mathfrak{v}_+ \leq \infty$, with moment generating function $\mathrm{M}_{\mathcal{V}}(u) := \mathbb{E}\left(\mathrm{e}^{u\mathcal{V}}\right)$ for all $u \in \mathcal{D}_{\mathcal{V}} := \{u \in \mathbb{R} : \mathbb{E}\left(\mathrm{e}^{u\mathcal{V}}\right) < \infty\} \supset (-\infty,0]$, and we further assume that $\mathcal{D}_{\mathcal{V}}$ contains at least an open neighborhood of the origin, namely, that $\mathfrak{m} := \sup\{u \in \mathbb{R} : \mathrm{M}_{\mathcal{V}}(u) < \infty\}$ belongs to $(0,\infty]$. Then clearly all positive moments of $\mathcal{V}$

exist. Existence and uniqueness of a solution to this stochastic system is guaranteed as soon as $\mathcal{V}$ admits a second moment [44, Chapter 5, Theorem 2.9]. Notice that the process (X, V) is not adapted to the filtration $(\mathcal{F}_t)_{t\geq 0}$ due to the lack of information on $\mathcal{V}$ in $\mathcal{F}_t$. The process is Markovian, however, with respect to the augmented filtration $\sigma(\mathcal{F}_t \vee \sigma(\mathcal{V}))_{t\geq 0}$.

When $\mathcal{V}$ is a Dirac distribution ($\mathfrak{v}_- = \mathfrak{v}_+$), system (2.1) corresponds to the standard Heston model [37], and it is well known that the stock price process $\exp(X)$ is a $\mathbb{P}$-martingale; it is trivial to check that this is still the case for (2.1). Behavior [51], asymptotics [25, 26, 27], and estimation and calibration [4, 51] of the Heston model have been treated at length in several papers, and we refer the interested reader to this literature for more details; we shall therefore always assume that $\mathfrak{v}_- < \mathfrak{v}_+$.

Remark 2.1. *For any $t \geq 0$, the tower property for conditional expectation yields*

$$\mathbb{E}(V_t) = \mathbb{E}[\mathbb{E}(V_t|\mathcal{V})] = \theta\left(1 - \mathrm{e}^{-\kappa t}\right) + \mathrm{e}^{-\kappa t}\mathbb{E}(\mathcal{V}),$$
$$\mathbb{V}(V_t) = \mathbb{E}[\mathbb{V}(V_t|\mathcal{V})] + \mathbb{V}[\mathbb{E}(V_t|\mathcal{V})] = \mathrm{e}^{-2\kappa t}\left(\mathbb{V}(\mathcal{V}) + \frac{\xi^2}{\kappa}\left(\mathrm{e}^{\kappa t} - 1\right)\mathbb{E}(\mathcal{V})\right) + \frac{\xi^2\theta}{2\kappa}\left(1 - \mathrm{e}^{-\kappa t}\right)^2.$$

Consider the standard Heston model ($\mathfrak{v}_- = \mathfrak{v}_+ =: V_0$) and construct $\mathcal{V}$ such that $\mathbb{E}(\mathcal{V}) = V_0$. Then, for any time $t \geq 0$, both random variables V_t (in (2.1) and in the standard Heston model) have the same expectation; however, the randomization of the initial variance increases the variance by $\mathrm{e}^{-2\kappa t}\mathbb{V}(\mathcal{V})$. As time tends to infinity, it is straightforward to show that the randomization preserves the ergodicity of the variance process, with a Gamma distribution as invariant measure, with identical mean and variance:

$$\lim_{t\uparrow\infty}\mathbb{E}(V_t) = \theta \qquad \text{and} \qquad \lim_{t\uparrow\infty}\mathbb{V}(V_t) = \frac{\xi^2\theta}{2\kappa}.$$

For any $t \geq 0$, let $\mathrm{M}(t,u)$ denote the moment generating function (mgf) of X_t:

$$\mathrm{M}(t,u) := \mathbb{E}\left(\mathrm{e}^{uX_t}\right) \qquad \text{for all } u \in \mathcal{D}_{\mathrm{M}}^t := \left\{u \in \mathbb{R} : \mathbb{E}\left(\mathrm{e}^{uX_t}\right) < \infty\right\}. \tag{2.2}$$

The tower property yields directly

$$\mathrm{M}(t,u) = \mathbb{E}\left(\mathrm{e}^{uX_t}\right) = \mathbb{E}\left(\mathbb{E}\left(\mathrm{e}^{uX_t}|\mathcal{V}\right)\right) = \mathbb{E}\left(\mathrm{e}^{\mathrm{C}(t,u)+\mathrm{D}(t,u)\mathcal{V}}\right) = \mathrm{e}^{\mathrm{C}(t,u)}\mathrm{M}_{\mathcal{V}}\left(\mathrm{D}(t,u)\right), \tag{2.3}$$

where the functions C and D arise directly from the (affine) representation of the mgf of the standard Heston model, recalled in Appendix A.1.

3. Practical appetizer and relation to model uncertainty.

3.1. The bounded support case: A practical appetizer. Before diving into the technical statements and proofs of asymptotic results in section 4, let us provide a numerical hors d'oeuvre, whetting the appetite of the reader regarding the practical relevance of the randomization. As mentioned in the introduction, the main drawback of classical continuous-path stochastic volatility models (without randomization and driven by standard Brownian motions) is that the small-maturity smile they generate is not steep enough to reflect the

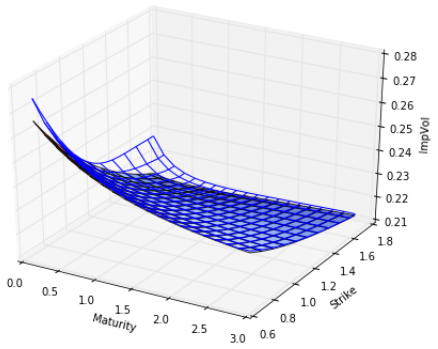

Figure 1. *Volatility surfaces of standard Heston (colored) and with randomization* $\mathcal{V} \overset{(Law)}{=} \mathcal{U}(4\%, 8.2\%)$.

reality of the market. The graph in Figure 1 represents a comparison of the implied volatility surface generated by the standard Heston model with

$$\kappa = 2.1, \qquad \theta = 0.05, \qquad V_0 = 0.06, \qquad \rho = -0.6, \qquad \xi = 0.1$$

and that of the Heston model randomized by a uniform distribution with $\mathfrak{v}_- = 0.04$ and $\mathfrak{v}_+ = 0.082$. From the trader's point of view, this could be understood as uncertainty on the actual value of V_0 (see also [29] for a related approach). Clearly, the randomization steepens the smile for small maturities, while its effect fades away as maturity becomes large. This numerical example intuitively yields the following informal conjecture.

Conjecture 3.1. *Under randomization of the initial volatility, the smile "explodes" for small maturities.*

We shall provide a precise formulation—and exact statements—of this conjecture. Despite appearances in Figure 1, the conjecture is actually false when the initial distribution has bounded support, such as in the uniform case here. However, as will be detailed in section 6.1, greater steepness of the smile (compared to the standard Heston model) does appear for a wide range of strikes, but not in the far tails (this, as well as the at-the-money curvature in the uncorrelated case, is quantified precisely in section 6.1). This leads us to believe that, even if an "explosion" does not actually occur in the bounded support case, this assumption may still be of practical relevance given the range of traded strikes.

4. Asymptotic behavior of the randomized model. This section is the core of the paper and relates the explosion of the implied volatility smile in small times to the tail behavior of the randomized initial variance. Section 4.1 (Proposition 4.1) provides the short-time behavior of the cumulant generating function (cgf) of the random sequence $(X_t)_{t\geq 0}$ and relates it to the choice of the initial distribution $\mathcal{V}$. This paves the way for a large deviations principle for the sequence $(X_t)_{t\geq 0}$. Section 4.2 concentrates on the case where both $\mathfrak{m}$ and $\mathfrak{v}_+$ are infinite: Theorem 4.5 indicates that the squared implied volatility has an explosion rate of t^γ with $\gamma \in (0, 1/2)$. The case where $\mathfrak{m} < \mathfrak{v}_+ = +\infty$ is covered in section 4.3, where an explosion rate of $\sqrt{t}$ is obtained. Section 4.4 provides the large-time asymptotic behavior of the implied volatility in our randomized setting; in particular, the long-term similarities between standard

and randomized Heston models are present in this section. Finally, section 4.5 covers the singular case of the small-time at-the-money implied volatility.

4.1. Preliminaries. As a first step in understanding the behavior of the implied volatility, we analyze the short-time limit of the rescaled cgf of the sequence $(X_t)_{t\geq 0}$. To do so, let $h : \mathbb{R}_+ \to \mathbb{R}_+$ be a smooth function, which can be extended at zero by continuity with $h(0) := \lim_{t\downarrow 0} h(t) = 0$. In light of (2.3), for any $t \geq 0$, we introduce the effective domain of the mgf of the rescaled random variable $X_t/h(t)$,

$$\mathcal{D}_t := \left\{ u \in \mathbb{R} : \mathrm{M}\left(t, \frac{u}{h(t)}\right) < \infty \right\},$$

as well as the following sets, for any $t > 0$:

$$\mathcal{D}^t_{\mathcal{V}} := \left\{ u \in \mathbb{R} : \mathrm{M}_{\mathcal{V}} \circ \mathrm{D}\left(t, \frac{u}{h(t)}\right) < \infty \right\}, \qquad \mathcal{D}^* := \liminf_{t\downarrow 0} \mathcal{D}_t = \bigcup_{t>0} \bigcap_{s\leq t} \mathcal{D}_s,$$
$$\mathcal{D}^*_{\mathcal{V}} := \liminf_{t\downarrow 0} \mathcal{D}^t_{\mathcal{V}} = \bigcup_{t>0} \bigcap_{s\leq t} \mathcal{D}^s_{\mathcal{V}}.$$

We now denote the pointwise limit $\Lambda_h(u) := \lim_{t\downarrow 0} \Lambda_h\left(t, u/h(t)\right)$, where

$$\Lambda_h\left(t, \frac{u}{h(t)}\right) := h(t) \log \mathrm{M}\left(t, \frac{u}{h(t)}\right). \tag{4.1}$$

The seemingly identical notation for the function and its pointwise limit should not create any confusion in this paper. Introduce further the real numbers $u_- \leq 0$ and $u_+ \geq 1$ and the function $\Lambda : (u_-, u_+) \to \mathbb{R}$:

$$\begin{cases} u_- := \dfrac{2}{\xi\overline{\rho}} \arctan\left(\dfrac{\overline{\rho}}{\rho}\right) \mathbf{1}_{\{\rho<0\}} - \dfrac{\pi}{\xi} \mathbf{1}_{\{\rho=0\}} + \dfrac{2}{\xi\overline{\rho}} \left(\arctan\left(\dfrac{\overline{\rho}}{\rho}\right) - \pi\right) \mathbf{1}_{\{\rho>0\}}, \\ u_+ := \dfrac{2}{\xi\overline{\rho}} \left(\arctan\left(\dfrac{\overline{\rho}}{\rho}\right) + \pi\right) \mathbf{1}_{\{\rho<0\}} + \dfrac{\pi}{\xi} \mathbf{1}_{\{\rho=0\}} + \dfrac{2}{\xi\overline{\rho}} \arctan\left(\dfrac{\overline{\rho}}{\rho}\right) \mathbf{1}_{\{\rho>0\}}, \\ \Lambda(u) := \dfrac{u}{\xi(\overline{\rho}\cot\left(\xi\overline{\rho}u/2\right) - \rho)}. \end{cases} \tag{4.2}$$

The following proposition, whose proof is postponed to Appendix D.1, summarizes the limiting behavior of $\Lambda_h(\cdot,\cdot)$ as t tends to zero. In view of Remark 4.2(ii) below, we shall only consider power functions of the type $h(t) \equiv ct^\gamma$. It is clear that there is no loss of generality by taking $c = 1$, as it only acts as a space-scaling factor. We shall therefore replace the notation Λ_h by Λ_γ to highlight the power exponent in action.

Proposition 4.1. *Let $h(t) = t^\gamma$, with $\gamma \in (0, 1]$. As t tends to zero, the following pointwise limit holds:*

$$\Lambda_\gamma(u) := \lim_{t\downarrow 0} \Lambda_\gamma\left(t, \frac{u}{t^\gamma}\right) = \begin{cases} 0, & u \in \mathbb{R}, & \text{if } \gamma \in (0, 1/2) & \text{for any } \mathcal{V}, \\ 0, & u \in \mathbb{R}, & \text{if } \gamma \in [1/2, 1), & \mathfrak{v}_+ < \infty, \\ \Lambda(u)\mathfrak{v}_+, & u \in (u_-, u_+), & \text{if } \gamma = 1, & \mathfrak{v}_+ < \infty, \\ \mathrm{L}_\pm \mathbf{1}_{\{u=\pm\sqrt{2\mathfrak{m}}\}}, & u \in [-\sqrt{2\mathfrak{m}}, \sqrt{2\mathfrak{m}}], & \text{if } \gamma = 1/2, & \mathfrak{v}_+ = \infty, \mathfrak{m} < \infty, \end{cases}$$

and is infinite elsewhere, where $\mathrm{L}_\pm \in [0,\infty]$. *Whenever* $\gamma > 1$ *(for any* $\mathcal{V}$*), or* $\mathfrak{m} < \infty$ *and* $\gamma > 1/2$*, the limit is infinite everywhere except at the origin.*

We shall call the (pointwise) limit *degenerate* whenever it is either equal to zero everywhere or zero at the origin and infinity everywhere else. In Proposition 4.1, only the last two cases are not degenerate.

Remark 4.2.

(i) *The case where* $\mathfrak{v}_+$ *and* $\mathfrak{m}$ *are both infinite is treated separately, in section 4.2, as more assumptions are needed on the behavior of the distribution of* $\mathcal{V}$.

(ii) *If* h *is not a power function, the proofs of Proposition 4.1 and Theorem 4.6 indicate that we only need to compare the order of* h *with orders of* $t^{1/2}$ *and* t. *Any nonpower function then yields degenerate limits.*

(iii) *In the last case,* $\mathrm{L}_\pm$ *depend on the explicit form of the mgf of* $\mathcal{V}$. *Example 6.2 illustrates this.*

When the random initial distribution $\mathcal{V}$ has bounded support ($\mathfrak{v}_+ < \infty$), Proposition 4.1 indicates that the only possible speed factor is $\gamma = 1$, and a direct application of the Gärtner–Ellis theorem (Theorem B.2) implies a large deviation for the sequence $(X_t)_{t\geq 0}$; adapting directly the methodology from [24], we obtain the small-time behavior of the implied volatility.

Corollary 4.3. *If* $\mathfrak{v}_+ < \infty$, *then* $X \sim \mathrm{LDP}_0(t, \Lambda^*_{\mathfrak{v}_+})$ *with* $\Lambda^*_{\mathfrak{v}_+}(x) := \sup\{ux - \Lambda(u)\mathfrak{v}_+ : u \in (u_-, u_+)\}$ *and*

$$\lim_{t\downarrow 0} \sigma_t^2(x) = \frac{x^2}{2\Lambda^*_{\mathfrak{v}_+}(x)} \qquad \text{for all } x \neq 0. \tag{4.3}$$

Approximations, in particular around the at-the-money $x = 0$, of the rate function $\Lambda^*_{\mathfrak{v}_+}$, and hence of the small-time implied volatility, can also be found in [24, Theorem 3.2] and apply here directly as well. Further, as discussed in detail in section 6.1, higher-order terms in the small-time expansion of $\sigma_t^2(x)$ can be obtained if the mgf of the initial randomization is known in closed form.

4.2. The thin-tail case. In the case $\mathfrak{m} = \infty$, Proposition 4.1 is not sufficient, as several different behaviors can occur. In this case, which we naturally coin "thin-tail," a more refined analysis is needed, and the following assumption shall be of utmost importance.

Assumption 4.4 (thin-tail). $\mathfrak{v}_+ = \infty$, *and* $\mathcal{V}$ *admits a smooth density* f *with* $\log f(v) \sim -l_1 v^{l_2}$ *as* v *tends to infinity for some* $(l_1, l_2) \in \mathbb{R}_+^* \times (1,\infty)$.

For notational convenience, we introduce the following two special rates of convergence, $\frac{1}{2} < \underline{\gamma} < 1 < \overline{\gamma}$, and two positive constants, $\underline{\mathfrak{c}}$, $\overline{\mathfrak{c}}$:

$$\underline{\gamma} := \frac{l_2}{1+l_2}, \qquad \overline{\gamma} := \frac{l_2}{l_2-1}, \qquad \underline{\mathfrak{c}} := (2l_1 l_2)^{\frac{1}{1+l_2}}, \qquad \overline{\mathfrak{c}} := (2l_1 l_2)^{\frac{1}{1-l_2}}. \tag{4.4}$$

The following theorem is the main result of this thin-tail section and provides both a large deviations principle for the log-stock price process as well as its implications on the small-maturity behavior of the implied volatility. Define the function $\underline{\Lambda}^* : \mathbb{R} \to \mathbb{R}_+$ by

$$\underline{\Lambda}^*(x) := \frac{\underline{\mathfrak{c}}}{2\underline{\gamma}} x^{2\underline{\gamma}} \qquad \text{for any } x \text{ in } \mathbb{R}. \tag{4.5}$$

Theorem 4.5. *Under Assumption 4.4, $X \sim \mathrm{LDP}_0(t^{\underline{\gamma}}, \underline{\Lambda}^*)$ with $\underline{\Lambda}^*$ given in (4.5), and, for any $x \neq 0$,*

$$\lim_{t \downarrow 0} t^{1-\underline{\gamma}} \sigma_t^2(x) = \underline{\mathfrak{c}}^{-1} \underline{\gamma} x^{2(1-\underline{\gamma})}.$$

In exponential Lévy models, the implied variance $\sigma_t^2(x)$ for nonzero x explodes at a rate of $|t \log t|$ [49, Proposition 4]. Theorem 4.5 implies that in a thin-tail randomized Heston model we have a much slower explosion rate of t^η with $\eta \in (0, 1/2)$. In [47] the authors commented that market data suggests that implied volatility with decreasing maturity still has a reasonable range of values and does not explode significantly, which might provide empirical grounds justifying the potential value of this randomized model as an alternative to the exponential Lévy models. The theorem relies on the study of the asymptotic behavior of the rescaled mgf of X_t.

Lemma 4.6. *Under Assumption 4.4, the only nondegenerate speed factor is $\gamma = \underline{\gamma}$, and*

$$\Lambda_{\underline{\gamma}}(u) = \frac{\overline{\mathfrak{c}}}{2\overline{\gamma}} u^{2\overline{\gamma}} \quad \text{for any } u \text{ in } \mathbb{R}. \tag{4.6}$$

Assumption 4.4 in particular implies that the function $\log f$ is regularly varying with index l_2 (which we denote by $|\log f| \in \mathcal{R}_{l_2}$; see also Appendix B.2 for a review of and useful results on regular variation). Without this slightly stronger assumption, however, the constant in (4.6)—essential to compute precisely the rate function governing the corresponding large deviations principle (Theorem 4.5)—would not be available. In order to prove the lemma and hence the theorem, let us first state and prove the following result.

Lemma 4.7. *If $|\log f| \in \mathcal{R}_l$ $(l > 1)$, then $\log \mathrm{M}_{\mathcal{V}}(z) \sim (l-1) \left(\frac{z}{l}\right)^{\frac{l}{l-1}} \psi(z)$ at infinity, with $\psi \in \mathcal{R}_0$ defined as*

$$\psi(z) := \left(\frac{z}{|\log f|^{\leftarrow}(z)} \right)^{\leftarrow} z^{\frac{l}{1-l}}.$$

Proof. Since $|\log f| \in \mathcal{R}_l$, Bingham's Lemma (Lemma B.4) implies $\log \mathbb{P}(\mathcal{V} \geq x) = \log \int_x^\infty \mathrm{e}^{\log f(y)} \mathrm{d}y \sim \log f(x)$, as x tends to infinity, and the result follows from Kasahara's Tauberian theorem [10, Theorem 4.12.7]. ∎

Proof of Lemma 4.6 and of Theorem 4.5. By Lemma B.5, the mgf of $\mathcal{V}$ is well defined on $\mathbb{R}_+$. Lemmas 4.7 and C.2 imply that as t tends to zero,

$$t^\gamma \log \mathrm{M}_{\mathcal{V}}\left(\mathrm{D}\left(t, \frac{u}{t^\gamma}\right)\right) = \begin{cases} t^\gamma \log \mathrm{M}_{\mathcal{V}}\left(\frac{u^2}{2} t^{1-2\gamma}\left(1 + \mathcal{O}\left(t^{1-\gamma}\right)\right)\right) \sim \frac{\overline{\mathfrak{c}}}{2\overline{\gamma}} u^{2\overline{\gamma}} t^{\overline{\gamma}(1-\gamma/\underline{\gamma})}, \text{ when } \gamma \in (1/2, 1), \\ t \log \mathrm{M}_{\mathcal{V}}\left(\frac{\Lambda(u)}{t}\left(1 + \mathcal{O}(t)\right)\right) \sim \frac{\overline{\mathfrak{c}}}{2\overline{\gamma}} 2^{\overline{\gamma}} \Lambda(u)^{\overline{\gamma}} t^{1-\overline{\gamma}}, \text{ when } \gamma = 1. \end{cases}$$

For $u \neq 0$ the right-hand side is well defined with nonzero limit if and only if $\gamma = \underline{\gamma} \in (1/2, 1)$; the case $\gamma = 1$ does not yield any nondegenerate behavior, and the lemma follows.

The large deviations principle stated in Theorem 4.5 is a direct consequence of Lemma 4.6 and the Gärtner–Ellis theorem (Theorem B.2), noting that the function $\Lambda_{\underline{\gamma}}$ in (4.6) satisfies all the required conditions and admits $\underline{\Lambda}^*$ as the Fenchel–Legendre transform. The translation of this asymptotic behavior into implied volatility follows along the same lines as in [24]. ∎

4.3. The fat-tail case. If $\mathfrak{v}_+$ is infinite and $\mathfrak{m}$ is finite, Proposition 4.1 states that the only choice for the rescaling factor is $h(t) = t^{1/2}$, but the form of the limiting rescaled cgf does not yield any immediate asymptotic estimates for the probabilities. In this case, we impose the following assumption on the mgf of $\mathcal{V}$ in the vicinity of the upper bound $\mathfrak{m}$ of its effective domain.

Assumption 4.8. *There exist* $(\gamma_0, \gamma_1, \gamma_2, \omega) \in \mathbb{R}^* \times \mathbb{R} \times \mathbb{R} \times \mathbb{N}^*_+$, *such that the following asymptotics hold for the cgf of* $\mathcal{V}$ *as* u *tends to* $\mathfrak{m}$ *from below:*

(4.7)
$$\log \mathrm{M}_{\mathcal{V}}(u) = \begin{cases} \gamma_0 \log(\mathfrak{m}-u) + \gamma_1 + o(1) & \text{for } \omega = 1, \gamma_0 < 0, \\ \dfrac{\gamma_0}{(\mathfrak{m}-u)^{\omega-1}} \{1 + \gamma_1(\mathfrak{m}-u)\log(\mathfrak{m}-u) + \gamma_2(\mathfrak{m}-u) + o(\mathfrak{m}-u)\} & \text{for } \omega \geq 2, \gamma_0 > 0 \end{cases}$$

and

(4.8)
$$\frac{\mathrm{M}'_{\mathcal{V}}(u)}{\mathrm{M}_{\mathcal{V}}(u)} = \begin{cases} \dfrac{|\gamma_0|}{\mathfrak{m}-u}\,(1+o(1)) & \text{for } \omega = 1, \gamma_0 < 0, \\ \dfrac{(\omega-1)\gamma_0}{(\mathfrak{m}-u)^{\omega}} \{1 + \mathfrak{a}(\mathfrak{m}-u)\log(\mathfrak{m}-u) + \mathfrak{b}(\mathfrak{m}-u) + o(\mathfrak{m}-u)\} & \text{for } \omega \geq 2, \gamma_0 > 0, \end{cases}$$

where $\mathfrak{a} := \gamma_1(\omega-2)(\omega-1)^{-1}$ *and* $\mathfrak{b} := [\gamma_2(\omega-2) - \gamma_1](\omega-1)^{-1}$.

Remark 4.9. *Condition* (4.8) *together with the expressions of* $\mathfrak{a}$ *and* $\mathfrak{b}$ *implies that the asymptotics of* $(\log(\mathrm{M}_{\mathcal{V}}))'$ *can be derived by differentiating* (4.7) *term by term. This is of course not always true; however, condition* (4.8) *is rather mild, and we shall check it directly in several cases where* $\mathrm{M}_{\mathcal{V}}$ *is known in closed form.*

Example 4.10.

- *For the exponential distribution with parameter* $\mathfrak{m}$, $(\gamma_0, \gamma_1, \omega) = (-1, \log \mathfrak{m}, 1)$.
- *For the noncentral* χ*-squared distribution as in Example 6.2,* $(\gamma_0, \gamma_1, \gamma_2, \omega) = \big(\frac{\lambda}{4}, -\frac{2q}{\lambda}, -2\big(1 + \frac{q}{\lambda}\log 2\big), 2\big)$.

For $\mathfrak{m} \in (0, \infty)$, introduce the function $\Lambda^* : \mathbb{R} \to \mathbb{R}_+$ as

$$\Lambda^*(x) := \sqrt{2\mathfrak{m}}|x|, \tag{4.9}$$

as well as, for any $t > 0$, the functions $\mathcal{E}_t, \mathcal{C}_t : \mathbb{R}^* \to \mathbb{R}^*_+$ by $\mathcal{E}_t(x) := \mathbf{1}_{\{\omega=1\}} + \exp\big(\frac{c_1(x)}{t^{1/4}}\big)\mathbf{1}_{\{\omega=2\}}$ and

$$\mathcal{C}_t(x) := \begin{cases} \exp\left(\dfrac{1}{2}(\rho\xi\mathfrak{m}+1)x + \gamma_1\right) \dfrac{|x|^{|\gamma_0|-1}}{\Gamma(|\gamma_0|)(2\mathfrak{m})^{1+|\gamma_0|/2}} t^{1-\frac{1}{2}|\gamma_0|} & \text{for } \omega = 1, \\ \exp\left(\dfrac{1}{2}(\rho\xi\mathfrak{m}+1)x + \gamma_0\gamma_2 + \dfrac{\gamma_0}{4\mathfrak{m}}\right) \dfrac{1}{2\mathfrak{m}\sqrt{2\pi}\zeta(x)} t^{\frac{7}{8}+\frac{1}{4}\gamma_0\gamma_1} & \text{for } \omega = 2, \end{cases} \tag{4.10}$$

where the functions c_1 and ζ are defined in Lemmas D.2 and D.3, respectively. Then the following behavior, proved in section D.2, holds for European option prices.

Theorem 4.11. *Under Assumption 4.8, European Call options with strike* e^x *have the following expansion:*

$$\mathbb{E}\big(\mathrm{e}^{X_t} - \mathrm{e}^x\big)^+ = (1-\mathrm{e}^x)^+ + \exp\left(-\frac{\Lambda^*(x)}{\sqrt{t}}\right)\mathcal{E}_t(x)\mathcal{C}_t(x)(1+o(1)) \quad \text{for any } x \neq 0, \text{ as } t \text{ tends to zero.}$$

Moreover, the small-time implied volatility behaves as follows whenever $x \neq 0$:

$$\sigma_t^2(x) = \frac{|x|}{2\sqrt{2\mathfrak{m}t}} + \begin{cases} \mathrm{h}_1^{(1)}(x) + \mathrm{h}_2^{(1)}\log(t) + o(1) & \text{for } \omega = 1, \\ \dfrac{c_1(x)}{4\mathfrak{m}t^{1/4}} + \mathrm{h}_1^{(2)}(x) + \mathrm{h}_2^{(2)}\log(t) + o(1) & \text{for } \omega = 2, \end{cases}$$

where

$$\mathrm{h}_1^{(1)}(x) := \frac{1}{4\mathfrak{m}}\left\{\frac{\rho\xi\mathfrak{m}}{2}x + \left(|\gamma_0| - \frac{1}{2}\right)\log|x| + \gamma_1 + \log(4\sqrt{\pi}) - \left(\frac{|\gamma_0|}{2} + \frac{1}{4}\right)\log(2\mathfrak{m}) - \log\Gamma(|\gamma_0|)\right\},$$

$$\mathrm{h}_1^{(2)}(x) := \frac{1}{4\mathfrak{m}}\left\{\frac{\rho\xi\mathfrak{m}}{2}x + \gamma_0\gamma_2 + \frac{9\gamma_0}{4\mathfrak{m}} + \frac{5}{8}\log 2 - \frac{3}{8}\log\mathfrak{m} + \frac{1}{4}\log\gamma_0 - \frac{1}{4}\log|x|\right\},$$

$$\mathrm{h}_2^{(1)} := \frac{1}{8\mathfrak{m}}\left(\frac{1}{2} - |\gamma_0|\right), \qquad \mathrm{h}_2^{(2)} := \frac{1}{16\mathfrak{m}}\left(\frac{1}{2} + \gamma_0\gamma_1\right), \quad c_1(x) \text{ defined as in Lemma D.2.}$$

A particular example of a randomization satisfying Assumption 4.8 is the noncentral χ-squared distribution. This case was the central focus of [39], where the small-time behavior of the forward smile in the Heston model was analyzed. As a sanity check, our Theorem 4.11 corresponds to [39, Theorem 4.1].

Corollary 4.12. *Under Assumption 4.8, for $\omega \leq 2$, $X \sim \mathrm{LDP}_0(\sqrt{t}, \Lambda^*)$.*

Remark 4.13. *Even though the leading order in the expansion is symmetric, Theorem 4.11 explains how the asymmetry in the volatility smile is generated. In particular, the term $\rho\xi x/8$ immediately shows how the leverage effect can be produced with $\rho < 0$.*

4.4. Large-time asymptotics. As observed in Figure 1, the effect of initial randomness decays when the maturity becomes large, so that the large-time behavior of the randomized Heston model should be similar to that of the standard Heston model, which has been discussed in detail in [25, 27, 38]. In the particular example of the forward Heston model—which coincides with randomizing with a noncentral χ-squared distribution—such a large-time behavior was analyzed in [40]. Throughout this section we assume $|\rho| < 1$ and $\kappa > \rho\xi$ (this condition usually holds on equity markets, where the instantaneous correlation ρ is negative—the so-called leverage effect), which guarantees the essential smoothness of the limiting cgf in a standard Heston as t tends to infinity, and define the function $\mathfrak{L}$ on $\mathbb{R}$ by

$$\mathfrak{L}(u) := \begin{cases} \dfrac{\kappa\theta}{\xi^2}\left(\kappa - \rho\xi u - d(u)\right) & \text{for } u \in [\overline{u}_-, \overline{u}_+], \\ +\infty & \text{for } u \in \mathbb{R} \setminus [\overline{u}_-, \overline{u}_+], \end{cases} \tag{4.11}$$

where $\overline{u}_\pm := \frac{1}{2\overline{\rho}^2\xi}\left(\xi - 2\kappa\rho \pm \sqrt{(\xi - 2\kappa\rho)^2 + 4\kappa^2\overline{\rho}^2}\right)$, and where the function d is given in (A.1). We further denote $\mathfrak{L}^*(x) := \sup_{u\in\mathbb{R}}\{ux - \mathfrak{L}(u)\}$, the convex conjugate of $\mathfrak{L}$. Forde and Jacquier [25, Theorem 2.1] proved that $\overline{u}_- < 0$ and $\overline{u}_+ > 1$. Consider now the following assumption.

Assumption 4.14. $\max\{\overline{u}_-(\overline{u}_- - 1), \overline{u}_+(\overline{u}_+ - 1)\} < \mathfrak{m}\xi^2 \leq \infty$.

Remark 4.15. *Assumption 4.14 is a technical one, needed to ensure that the limiting cgf of the randomized model is essentially smooth. Should it break down, a more refined analysis,*

similar to the one in [40], *could be carried out to prove large deviations, but we leave this for future research.*

Theorem 4.16. *Under Assumption* 4.14, $(t^{-1}X_t) \sim \mathrm{LDP}_\infty(t^{-1}, \mathfrak{L}^*)$ *and*

$$\lim_{t\uparrow\infty} \sigma_t^2(xt) = \begin{cases} 2\left(2\mathfrak{L}^*(x) - x + 2\sqrt{\mathfrak{L}^*(x)(\mathfrak{L}^*(x)-x)}\right) & \text{for } x \in \left(-\frac{\theta}{2}, \frac{\overline{\theta}}{2}\right), \\ 2\left(2\mathfrak{L}^*(x) - x - 2\sqrt{\mathfrak{L}^*(x)(\mathfrak{L}^*(x)-x)}\right) & \text{for } x \in \mathbb{R} \setminus \left[-\frac{\theta}{2}, \frac{\overline{\theta}}{2}\right], \end{cases}$$

where $\overline{\theta} := \frac{\kappa\theta}{\kappa - \rho\xi} > 0$. *If* $x \in \left\{-\frac{\theta}{2}, \frac{\overline{\theta}}{2}\right\}$, *then* $\lim_{t\uparrow\infty} \sigma_t^2\left(\frac{\overline{\theta}t}{2}\right) = \overline{\theta}$ *and* $\lim_{t\uparrow\infty} \sigma_t^2\left(-\frac{\theta t}{2}\right) = \theta$.

Remark 4.17.

- *As proved in* [25], *the map* $x \mapsto \mathfrak{L}^*(x) - x$ *is smooth and strictly convex, it attains its minimum at the point* $\overline{\theta}/2$, *and* $\mathfrak{L}^*(\overline{\theta}/2) - \overline{\theta}/2 = \mathfrak{L}^*(\overline{\theta}/2)' - 1 = 0$.
- *Theorem* 4.16 *has the same form as* [25, Corollary 2.4], *confirming the similar large-time behaviors of the classical and the randomized Heston models.*
- *Higher-order terms can be derived using the saddle point method described in detail in* [27] *(see also* [40, Proposition 2.12]*).*

Theorem 4.16 provides the large-time behavior of the implied volatility smile with a time-dependent strike. For fixed strike, the initial randomization has no effect, and we recover the flattening effect of the smile.

Corollary 4.18 (fixed strike). *Under Assumption* 4.14,

$$\lim_{t\uparrow\infty} \sigma_t^2(x) = 8\mathfrak{L}^*(0) = \frac{4\kappa\theta}{\xi^2(1-\rho^2)}\left(-2\kappa + \rho\xi + \sqrt{\xi^2 + 4\kappa^2 - 4\kappa\rho\xi}\right) \qquad \text{for all } x \in \mathbb{R}.$$

4.5. At-the-money case. All our small-maturity results above hold in the out-of-the-money case $x \neq 0$. As usual in the literature on implied volatility asymptotics, the at-the-money case exhibits radically different behavior, and a separate analysis is needed. We first recall in Lemma 4.19 the at-the-money asymptotics in the classical Heston model [26]. To differentiate between standard and randomized Heston models, denoting by $\sigma_t(x, v_0)$ the implied volatility in the standard Heston model with fixed initial condition $V_0 = v_0 > 0$.

Lemma 4.19 (see [26, Corollary 4.4]). *In the standard Heston model with* $V_0 = v_0 > 0$, *assume that there exists* $\varepsilon > 0$ *such that the map* $(t, x) \mapsto \sigma_t^2(x, v_0)$ *is of class* $\mathcal{C}^{1,1}([0, \varepsilon) \times (-\varepsilon, \varepsilon))$. *Then* $\sigma_t^2(0, v_0) = v_0 + a(v_0)t + o(t)$, *where* $a(v_0) := -\frac{1}{12}\xi^2\left(1 - \frac{1}{4}\rho^2\right) + \frac{1}{4}v_0\rho\xi + \frac{1}{2}\kappa(\theta - v_0)$.

Theorem 4.20. *In a randomized Heston model,* $\sigma_t(0) = \mathbb{E}(\sqrt{\mathcal{V}}) + o(1)$ *holds as time tends to zero.*

Proof. Since $\mathfrak{m} \in (0, \infty]$, then $\mathbb{E}(\sqrt{\mathcal{V}})$ is finite. Denote by $\mathrm{C_{BS}}(t, x, \Sigma)$ the European Call option price in the Black–Scholes model with maturity t, strike e^x, and volatility Σ, and denote by $\mathrm{C_H}(t, x, v)$ its price in the standard Heston model with $V_0 = v$. Using the tower property,

$$\mathbb{E}\left(\mathrm{e}^{X_t} - 1\right)^+ = \mathbb{E}\left(\mathbb{E}\left(\mathrm{e}^{X_t} - 1\right)^+ | \mathcal{V}\right) = \mathbb{E}\left(\mathrm{C_H}(t, 0, \mathcal{V})\right), \tag{4.12}$$

and Lemma 4.19 and [26, Corollary 4.5] imply that the equation $\mathrm{C_H}\big(t,0,\mathcal{V}\big) = \mathrm{C_{BS}}\big(t,0,\sqrt{\mathcal{V}+a(\mathcal{V})t}\big)\big(1+o(1)\big)$ holds $\mathbb{P}$-almost surely. Also for any $c\in\mathbb{R}$, [26, Proposition 3.4] implies that

$$\mathrm{C_{BS}}\left(t,0,\sqrt{\Sigma^2+ct}\right) = \frac{1}{\sqrt{2\pi}}\left(\Sigma t^{1/2} + \frac{12c/\Sigma-\Sigma^4}{24\Sigma}t^{3/2} + \mathcal{O}\left(t^{5/2}\right)\right).$$

Plugging these equations back into (4.12) and equating (4.12) with $\mathrm{C_{BS}}\left(t,0,\sigma_t(0)\right)$, the theorem follows from

$$\sqrt{\frac{t}{2\pi}}\mathbb{E}\left\{\left(\sqrt{\mathcal{V}}+\frac{12a(\mathcal{V})-\mathcal{V}^{5/2}}{24\mathcal{V}}t+\mathcal{O}\left(t^2\right)\right)\left(1+o(1)\right)\right\} = \sqrt{\frac{t}{2\pi}}\left(\sigma_t(0)-\frac{\sigma_t^3(0)}{24}t+\mathcal{O}\left(t^2\right)\right). \quad \blacksquare$$

Remark 4.21. *If $\mathbb{E}(\mathcal{V}^{-1/2})$ is finite, then following a similar procedure we obtain higher-order terms of $\sigma_t(0)$,*

$$\sigma_t(0) = \mathbb{E}(\sqrt{\mathcal{V}}) + \left\{\mathfrak{c}_1\mathbb{E}(\mathcal{V}^{-1/2}) + \mathfrak{c}_2\mathbb{E}(\sqrt{\mathcal{V}}) + \mathfrak{c}_3\left(\mathbb{E}(\sqrt{\mathcal{V}})^3 - \mathbb{E}(\mathcal{V}^{3/2})\right)\right\}t + o(t),$$

where $\mathfrak{c}_1 := \frac{1}{4}(\kappa\theta+\xi^2(\rho^2-4)/24)$, $\mathfrak{c}_2 := \frac{1}{8}(\rho\xi-2\kappa)$, and $\mathfrak{c}_3 := \frac{1}{24}$. In the noncentral χ-squared case we recover the result of [39, Theorem 4.4].

5. A dynamic pricing framework. The model proposed in this paper has so far only been studied in a static way, namely, from the inception time of the (European contract), with a view towards calibration of the implied volatility surface. Although it provides a better fit to short-maturity options by steepening the skew, it is not obvious how to use the model dynamically; in particular, it is unclear how to choose the random initial value of the volatility process during the life of the contract, should one wish to sell or buy the option, or for hedging purposes. Mathematically, assume that at time zero the trader chooses an initial randomization $\mathcal{V}$ (or classically a Dirac mass at some positive point), and suppose that at some later time $\breve{t}>0$ she needs to reprice the option (with retaining the maturity τ). How should she choose the new initial random variable $\mathcal{V}_{\breve{t}}$? Since the variance process has continuous paths, a suitable choice of $\mathcal{V}_{\breve{t}}$, consistent with the dynamics of the variance, is obviously $V_{\breve{t}}$, the solution of the SDE (2.1), after running it from time zero to time $\breve{t}$. With an initial guess $\mathcal{V}$ at time zero, then, at time $\breve{t}$, conditional on $\mathcal{V}$, $\mathcal{V}_{\breve{t}}$ is distributed as $\beta_{\breve{t}}\chi^2(q,\lambda)$, where $\beta_{\breve{t}} := \xi^2(1-\mathrm{e}^{-\kappa\breve{t}})/(4\kappa)$, and $\chi^2(q,\lambda)$ is a noncentral χ-squared distribution with $q := 4\kappa\theta/\xi^2$ degrees of freedom and noncentrality parameter $\lambda := 4\kappa\mathcal{V}/(\xi^2(\mathrm{e}^{\kappa\breve{t}}-1))$. From the tower property, the moment generating function of $\mathcal{V}_{\breve{t}}$ then reads

$$\mathrm{M}_{\mathcal{V}_{\breve{t}}}(u) = \mathbb{E}\left[\mathbb{E}\left(\mathrm{e}^{uV_{\breve{t}}}|\mathcal{V}\right)\right] = (1-2\beta_{\breve{t}}u)^{-q/2}\,\mathrm{M}_{\mathcal{V}}\left(\frac{\exp(-\kappa\breve{t})u}{1-2\beta_{\breve{t}}u}\right) \tag{5.1}$$

for all $u\in\mathcal{D}^H_{\breve{t}} = \{u\in\mathbb{R} : \mathrm{M}_{\mathcal{V}_{\breve{t}}}(u)<\infty\}$. Setting $\mathfrak{b}_t := 1/(2\beta_{\breve{t}})$, we have

$$\begin{aligned}\mathcal{D}^H_{\breve{t}} &= (-\infty,\mathfrak{b}_{\breve{t}})\bigcap\left\{u\in\mathbb{R} : \frac{\exp(-\kappa\breve{t})u}{1-2\beta_{\breve{t}}u}\in\mathcal{D}_{\mathcal{V}}\right\}\\ &= \begin{cases}(-\infty,\mathfrak{b}_{\breve{t}}) & \text{if } \mathfrak{m}=\infty,\\ (-\infty,\mathfrak{b}_{\breve{t}})\bigcap\left(-\infty,\dfrac{\mathfrak{m}}{\mathrm{e}^{-\kappa\breve{t}}+2\beta_{\breve{t}}\mathfrak{m}}\right) = (-\infty,\mathfrak{b}^*_{\breve{t}}) & \text{if } \mathfrak{m}<\infty,\end{cases}\end{aligned}$$

where $\mathfrak{b}^*_{\breve{t}} := \frac{\mathfrak{m}\mathfrak{b}_{\breve{t}}}{\mathfrak{m}+\mathfrak{b}_{\breve{t}}\exp(-\kappa\breve{t})}$. We now discuss the impact of different choices of $\mathcal{V}$ at time zero on the distribution of $\mathcal{V}_{\breve{t}}$ and on the implied variance $\sigma^2_\tau(x,\breve{t})$ at time $\breve{t}$ (for a remaining maturity τ). We keep here the terminology introduced in section 4 regarding the tail behavior of $\mathcal{V}$.

Before diving into the detailed analysis, we argue that $\mathcal{V}_{\breve{t}}$ chosen this way should only serve as a candidate for the initial distribution at time $\breve{t}$ and in practice should be recalibrated according to updated (noisy) market observations at time $\breve{t}$. Market noises explain how the distribution of $\mathcal{V}_{\breve{t}}$ can deviate from the ergodic distribution: the impact of the (instantaneous) noises can change the shape and parameterization of the randomization. We further comment that understanding the choice of $\mathcal{V}_{\breve{t}}$ is also useful from a model risk point of view: at time zero, it is important to understand and simulate the behaviors of model parameters at a given future time. We show in this section, in our setting, that $\mathcal{V}_{\breve{t}}$ can in fact only be fat tailed, and therefore, for consistency, one should probably start with $\mathcal{V}$ in the class of fat-tail distributions.

5.1. The bounded-support case. In this case, $\mathcal{D}^H_{\breve{t}} = (-\infty, \mathfrak{b}_{\breve{t}})$; the proof of Proposition 4.1 showed that $\lim_{u\uparrow\infty} u^{-1}\log \mathrm{M}_{\mathcal{V}}(u) = \mathfrak{v}_+$. Combining this with (5.1), we obtain, as u tends to $\mathfrak{b}_{\breve{t}}$ from below,

$$\begin{aligned}\log \mathrm{M}_{\mathcal{V}_{\breve{t}}}(u) &= -\frac{q}{2}\log(1-2\beta_{\breve{t}}u) + \frac{\mathrm{e}^{-\kappa\breve{t}}\mathfrak{v}_+ u}{1-2\beta_{\breve{t}}u}\,(1+o(1)) \\ &= \frac{q}{2}\log\left(\frac{\mathfrak{b}_{\breve{t}}}{\mathfrak{b}_{\breve{t}}-u}\right) + \frac{\mathrm{e}^{-\kappa\breve{t}}\mathfrak{v}_+\mathfrak{b}_{\breve{t}}u}{\mathfrak{b}_{\breve{t}}-u}(1+o(1)) = \frac{\mathrm{e}^{-\kappa\breve{t}}\mathfrak{v}_+\mathfrak{b}^2_{\breve{t}}}{\mathfrak{b}_{\breve{t}}-u}\,(1+o(1))\,,\end{aligned}$$

so that, at leading order, $\mathcal{V}_{\breve{t}}$ behaves asymptotically as a fat-tail distribution as in Assumption 4.8 with $\omega = 2$. In the particular case of a uniform distribution on $[\mathfrak{v}_-, \mathfrak{v}_+] \subset [0,\infty)$, as u tends to $\mathfrak{b}_{\breve{t}}$ from below, we obtain

$$\begin{aligned}&\log \mathrm{M}_{\mathcal{V}_{\breve{t}}}(u) \\ &= \frac{q}{2}\log\left(\frac{\mathfrak{b}_{\breve{t}}}{\mathfrak{b}_{\breve{t}}-u}\right) + \mathfrak{b}_{\breve{t}}\mathfrak{v}_+\mathrm{e}^{-\kappa\breve{t}}\left(\frac{\mathfrak{b}_{\breve{t}}}{\mathfrak{b}_{\breve{t}}-u}-1\right) + \log\left(\frac{1-\exp\{(\mathfrak{v}_- - \mathfrak{v}_+)\mathrm{e}^{-\kappa\breve{t}}\mathfrak{b}_{\breve{t}}u/(\mathfrak{b}_{\breve{t}}-u)\}}{\mathrm{e}^{-\kappa\breve{t}}\mathfrak{b}_{\breve{t}}u(\mathfrak{v}_+-\mathfrak{v}_-)}(\mathfrak{b}_{\breve{t}}-u)\right) \\ &= \frac{\mathrm{e}^{-\kappa\breve{t}}\mathfrak{b}^2_{\breve{t}}\mathfrak{v}_+}{\mathfrak{b}_{\breve{t}}-u}\left[1+\frac{\mathrm{e}^{\kappa\breve{t}}(2-q)}{2\mathfrak{b}^2_{\breve{t}}\mathfrak{v}_+}(\mathfrak{b}_{\breve{t}}-u)\log(\mathfrak{b}_{\breve{t}}-u) + \left\{\frac{\mathrm{e}^{\kappa\breve{t}}}{\mathfrak{b}_{\breve{t}}\mathfrak{v}_+}\log\left(\frac{\mathrm{e}^{\kappa\breve{t}}\mathfrak{b}^{q/2-2}_{\breve{t}}}{\mathfrak{v}_+-\mathfrak{v}_-}\right)-1\right\}\frac{\mathfrak{b}_{\breve{t}}-u}{\mathfrak{b}_{\breve{t}}} + o(\mathfrak{b}_{\breve{t}}-u)\right].\end{aligned}$$

Hence in a uniform randomization environment, at future time $\breve{t}$, the shape of the distribution of $\mathcal{V}_{\breve{t}}$ depends both on $\mathcal{V}$ and on the parameters κ, θ, ξ that control the dynamics of the variance process. Moreover, from Theorem 4.11, the implied variance at time $\breve{t}$, denoted by $\sigma^2_\tau(x,\breve{t})$, has an explosion rate of $\sqrt{\tau}$:

$$\sigma^2_\tau(x,\breve{t}) = \frac{|x|\tau^{-1/2}}{2\sqrt{2\mathfrak{b}_{\breve{t}}}} + \frac{\sqrt{\mathfrak{v}_+|x|}}{2\mathrm{e}^{\kappa\breve{t}/2}}(2\mathfrak{b}_{\breve{t}}\tau)^{-1/4} + o\left(\tau^{-1/4}\right) \quad \text{for all } x\neq 0, \text{ as } \tau \text{ tends to zero.}$$

5.2. The thin-tail case (Assumption 4.4). Here again, $\mathcal{D}_{\breve{t}}^H = (-\infty, \mathfrak{b}_{\breve{t}})$, and applying Lemma 4.7 with $\log f \sim -l_1 v^{l_2}$, we have

$$\begin{aligned}\log \mathrm{M}_{\mathcal{V}_{\breve{t}}}(u) &= \frac{q}{2}\log\left(\frac{\mathfrak{b}_{\breve{t}}}{\mathfrak{b}_{\breve{t}}-u}\right) + l_1(l_2-1)\left(\frac{1}{l_1 l_2}\right)^{\frac{l_2}{l_2-1}}\left(\frac{\mathrm{e}^{-\kappa\breve{t}}\mathfrak{b}_{\breve{t}}^2}{\mathfrak{b}_{\breve{t}}-u}\right)^{\frac{l_2}{l_2-1}}(1+o(1)) \\ &= \frac{q}{2}\log\left(\frac{\mathfrak{b}_{\breve{t}}}{\mathfrak{b}_{\breve{t}}-u}\right) + \frac{2^{\overline{\gamma}-1}\overline{\mathfrak{c}}}{\overline{\gamma}}\left(\frac{\mathrm{e}^{-\kappa\breve{t}}\mathfrak{b}_{\breve{t}}^2}{\mathfrak{b}_{\breve{t}}-u}\right)^{\overline{\gamma}}(1+o(1))\,, \end{aligned} \tag{5.2}$$

as u tends to $\mathfrak{b}_{\breve{t}}$ from below, so that a thin-tail initial randomization generates a fat-tail distribution for $\mathcal{V}_{\breve{t}}$ at time $\breve{t}$. In light of (5.2), Assumption 4.8 does not hold, and hence $\mathcal{V}_{\breve{t}}$ is neither of Gamma nor of noncentral χ-squared type. A case-by-case analysis depending on the distribution of $\mathcal{V}$ is therefore needed in order to make the $o(\cdot)$ term in (5.2) more precise.

Example 5.1 (folded-Gaussian randomization). *When $f(v) \equiv \mathfrak{c}\mathrm{e}^{-l_1 v^2}$, straightforward computations yield*

$$\begin{aligned}\log \mathrm{M}_{\mathcal{V}_{\breve{t}}}(u) &= \frac{q}{2}\log\left(\frac{\mathfrak{b}_{\breve{t}}}{\mathfrak{b}_{\breve{t}}-u}\right) + \frac{1}{4l_1}\left(\frac{\mathrm{e}^{-\kappa\breve{t}}\mathfrak{b}_{\breve{t}}u}{\mathfrak{b}_{\breve{t}}-u}\right)^2 + \log\left(\mathfrak{c}\sqrt{\frac{\pi}{l_1}}\right) + \log\left(\frac{1}{2}+\Phi\left(\frac{\mathrm{e}^{-\kappa\breve{t}}\mathfrak{b}_{\breve{t}}u}{\sqrt{2l_1}(\mathfrak{b}_{\breve{t}}-u)}\right)\right) \\ &=: \frac{\mathfrak{c}_0}{(\mathfrak{b}_{\breve{t}}-u)^2} + \frac{\mathfrak{c}_1}{\mathfrak{b}_{\breve{t}}-u} + \mathfrak{c}_2 - \frac{q}{2}\log(\mathfrak{b}_{\breve{t}}-u) + o(1).\end{aligned}$$

We can obtain the small-time asymptotic expansion of the option price using an approach similar to the proof of Theorem 4.11. Specifically, only Lemma D.3 needs to be adjusted, and the rescaling factor is now $\vartheta(\tau) = \tau^{1/6}$; the main contribution to the asymptotics of out-of-the-money option prices is still given in Lemma D.2. Translating this into the asymptotics of the implied variance, we obtain, for small τ,

$$\sigma_\tau^2(x,\breve{t}) = \frac{|x|}{2\sqrt{2\mathfrak{b}_{\breve{t}}\tau}} + \frac{2|x|^{2/3}}{3(4l_1)^{1/3}}\frac{\exp\left(-\frac{2\kappa\breve{t}}{3}\right)}{\tau^{1/3}} + o(\tau^{-1/3}).$$

5.3. The fat-tail case. In this case, $\mathcal{D}_{\breve{t}}^H = (-\infty, \mathfrak{b}_{\breve{t}}^*)$. Here we only discuss two special cases for $\mathcal{V}$: the Gamma distribution, and the (scaled) noncentral χ-squared distribution.

Example 5.2 (Gamma randomization). *If $\mathcal{V} \overset{(Law)}{=} \Gamma(\alpha, \mathfrak{m})$, then from (5.1) we have*

$$\begin{aligned}\log \mathrm{M}_{\mathcal{V}_{\breve{t}}}(u) &= \frac{q}{2}\log\left(\frac{\mathfrak{b}_{\breve{t}}}{\mathfrak{b}_{\breve{t}}-u}\right) - \alpha\log\left(1-\frac{\mathrm{e}^{-\kappa\breve{t}}u\mathfrak{b}_{\breve{t}}}{\mathfrak{m}(\mathfrak{b}_{\breve{t}}-u)}\right) = -\alpha\log\left(\frac{\mathfrak{m}\mathfrak{b}_{\breve{t}} - (\mathfrak{m}+\exp(-\kappa\breve{t})\mathfrak{b}_{\breve{t}})u}{\mathfrak{m}(\mathfrak{b}_{\breve{t}}-u)}\right) \\ &= -\alpha\log(\mathfrak{b}_{\breve{t}}^*-u) + \alpha\log\left(\frac{\mathfrak{m}(\mathfrak{b}_{\breve{t}}-u)}{\mathfrak{m}+\exp(-\kappa\breve{t})\mathfrak{b}_{\breve{t}}}\right) + \frac{q}{2}\log\left(\frac{\mathfrak{b}_{\breve{t}}}{\mathfrak{b}_{\breve{t}}-u}\right).\end{aligned}$$

Consequently $\mathcal{V}_{\breve{t}}$ is still a fat-tail distribution satisfying Assumption 4.8 with $\omega = 1$, $\gamma_0 = -\alpha$, while the upper bound of the support of the mgf now depends on both the initial distribution $\mathcal{V}$

and the evolution of the process (through $\mathfrak{b}^*_{\breve{t}}$*). A direct application of Theorem 4.11 further suggests that, for small enough* $\tau > 0$*,*

$$\sigma^2_\tau(x,\breve{t}) = \frac{|x|}{2\sqrt{2\mathfrak{b}^*_{\breve{t}}\tau}} + \mathrm{h}^{(1)}_1(x) + \mathrm{h}^{(1)}_2 \log(\tau) + o(1), \qquad \textit{with } \mathrm{h}^{(1)}_1, \mathrm{h}^{(1)}_2 \textit{ given in Theorem 4.11.}$$

Example 5.3 (noncentral χ^2 randomization). *If* $\mathcal{V} \overset{(Law)}{=} \alpha\chi^2(\mathfrak{a},\mathfrak{b})$*, then* $\mathfrak{m} = 1/(2\alpha)$*, and*

$$\begin{aligned}
\log \mathrm{M}_{\mathcal{V}_{\breve{t}}}(u) &= \frac{q}{2}\log\left(\frac{\mathfrak{b}_{\breve{t}}}{\mathfrak{b}_{\breve{t}} - u}\right) + \left(\frac{\alpha\mathfrak{b}z}{1-2\alpha z} - \frac{\mathfrak{a}}{2}\log(1-2\alpha z)\right)\Big|_{z=\exp(-\kappa\breve{t})u/(1-2\beta_{\breve{t}}u)} \\
&= \frac{\alpha \mathrm{e}^{-\kappa\breve{t}}\mathfrak{b}\mathfrak{b}^*_{\breve{t}}u}{\mathfrak{b}^*_{\breve{t}} - u} - \frac{\mathfrak{a}}{2}\log\left(\frac{\mathfrak{b}_{\breve{t}}(\mathfrak{b}^*_{\breve{t}} - u)}{\mathfrak{b}^*_{\breve{t}}(\mathfrak{b}_{\breve{t}} - u)}\right) + \frac{q}{2}\log\left(\frac{\mathfrak{b}_{\breve{t}}}{\mathfrak{b}_{\breve{t}} - u}\right) \\
&= \frac{\alpha \mathrm{e}^{-\kappa\breve{t}}\mathfrak{b}\mathfrak{b}^{*2}_{\breve{t}}}{\mathfrak{b}^*_{\breve{t}} - u} - \frac{\mathfrak{a}}{2}\log(\mathfrak{b}^*_{\breve{t}} - u) + \frac{q-\mathfrak{a}}{2}\log\left(\frac{\mathfrak{b}_{\breve{t}}}{\mathfrak{b}_{\breve{t}} - \mathfrak{b}^*_{\breve{t}}}\right) + \frac{\mathfrak{a}}{2}\log\mathfrak{b}^*_{\breve{t}} - \alpha\mathrm{e}^{-\kappa\breve{t}}\mathfrak{b}\mathfrak{b}^*_{\breve{t}} + \mathcal{O}(\mathfrak{b}^*_{\breve{t}} - u),
\end{aligned}$$

which satisfies (4.7) in Assumption 4.8 with $\omega = 2$ *as* u *tends to* $\mathfrak{b}^*_{\breve{t}}$*, with* $\mathfrak{b}^*_{\breve{t}}$ *playing the role of the boundary* $\mathfrak{m}$*, and* $\gamma_0 = \alpha\mathfrak{b}\mathfrak{b}^{*2}_{\breve{t}}\mathrm{e}^{-\kappa\breve{t}}$*. As a result, the implied variance* $\sigma^2_\tau(x,\breve{t})$ *has an explosion rate of* $\sqrt{\tau}$ *as* τ *tends to zero, and its full asymptotic expansion is provided in Theorem 4.11.*

This analysis shows that a suitable choice for $\mathcal{V}_{\breve{t}}$, consistent with the dynamics of the variance process, can actually depend on the initial randomization at time zero, as well as the evolution of the variance. Even though all three types of initial randomization imply a fat-tail initial distribution at future time, the generated small remaining-maturity implied volatility smiles are very different. The folded-Gaussian (thin tail) generates a steeper smile compared to the bounded support case; a fat-tail distribution for $\mathcal{V}$ generates an even steeper volatility smile at τ, since the coefficient of the leading order is $\mathfrak{b}^*_{\breve{t}}$, which is strictly less than $\mathfrak{b}_{\breve{t}}$.

Remark 5.4. *All distributions discussed in section 4 generate a fat-tail distribution for* $\mathcal{V}_{\breve{t}}$*. However, should the assumptions in section 4 break down, this may no longer be true: Equation (5.1) suggests that the mgf of* $\mathcal{V}_{\breve{t}}$ *can be ill-defined whenever that of* $\mathcal{V}$ *does not exist—in the case of a Cauchy distribution, for example. That said, the study of the effective domain below (5.1) indicates that, in our setting, only fat-tail distributions for* $\mathcal{V}_{\breve{t}}$ *are possible.*

Remark 5.5. *As* $\breve{t}$ *tends to zero,* $\beta_{\breve{t}}$ *also converges to zero,* $\mathfrak{b}_{\breve{t}}$ *diverges to infinity, and* $\mathfrak{b}^*_{\breve{t}}$ *tends to* $\mathfrak{m}$ *(defined on Page 101). Plugging these into the asymptotic behavior developed in section 5, we recover the moment generating functions from section 4 as well as the asymptotics of the implied variance.*

6. Examples and numerics. We now choose some common distributions supported on a subset of $[0,\infty)$ for the initial randomization to illustrate the results in section 4. We first start with the bounded support case and provide rigorous justification for the statements in section 3. In section 6.1, we consider a uniformly distributed initial variance, with $\mathfrak{v}_+$ finite, and provide full asymptotics of European Call prices. The remaining sections are devoted to the unbounded support case; specifically, sections 6.2–6.4 correspond to the fat-tail case,

so that Theorem 4.11 can be applied. The thin-tail environment is illustrated in section 6.3, where the initial distribution satisfies Assumption 4.4 with $l_2 = 2$.

6.1. Uniform randomization. Assume that $\mathcal{V}$ is uniformly distributed on $[\mathfrak{v}_-, \mathfrak{v}_+]$ with $0 \leq \mathfrak{v}_- < \mathfrak{v}_+ < \infty$. Then Corollary 4.3 provides the leading term of short-time implied volatility. However, as will be shown in section 6.6, the true volatility smile for small t is much steeper compared with the leading term, so that higher-order terms shall be considered. For any $x \neq 0$, denote by $u^*_{\mathfrak{v}_+}(x)$ the unique solution in (u_-, u_+) to the equation $x = \Lambda'(u)\mathfrak{v}_+$, with Λ described in (4.2). From [26, Remark 2.1], existence and uniqueness of such a solution are straightforward, and $u^*_{\mathfrak{v}_+}(x) \neq 0$ holds for any nonzero x. Introduce the function $\mathrm{U} : \mathbb{R}^* \to \mathbb{R}^*_+$ by

$$\mathrm{U}_{\mathfrak{v}_+}(x) := \exp\left\{\mathrm{D}^0_0(u^*_{\mathfrak{v}_+}(x))\mathfrak{v}_+ + \mathrm{C}_0(u^*_{\mathfrak{v}_+}(x)) + x\right\}, \tag{6.1}$$

where the functions D^0_0 and C_0 are provided in (C.1)–(C.2). From [26, Remark 3.2], the function U is well defined on $\mathbb{R}^*$. The following theorem is the main result of this section and provides a detailed asymptotic behavior of call option prices as the maturity becomes small.

Theorem 6.1. *Under uniform randomization, as t decreases to zero, European Call option prices behave as*

$$\mathbb{E}\left(\mathrm{e}^{X_t} - \mathrm{e}^x\right)^+ = (1 - \mathrm{e}^x)^+ + \exp\left(-\frac{\Lambda^*_{\mathfrak{v}_+}(x)}{t}\right) \frac{\mathrm{U}_{\mathfrak{v}_+}(x) t^{5/2}\,(1 + o(1))}{(\mathfrak{v}_+ - \mathfrak{v}_-)\Lambda(u^*_{\mathfrak{v}_+}(x)) u^*_{\mathfrak{v}_+}(x)^2 \sqrt{2\pi\mathfrak{v}_+ \Lambda''(u^*_{\mathfrak{v}_+}(x))}}$$

for any $x \neq 0$,

where the function $\Lambda^*_{\mathfrak{v}_+}$ was introduced in Corollary 4.3.

Remark 6.2.

- *The remainder is of order $t^{5/2}$, instead of $t^{3/2}$, as in both standard Heston and Black–Scholes models [26]. This can also be seen at the level of the (asymptotic behavior of) corresponding densities, as noted in Remark 6.3 below.*
- *The asymptotics holds locally for any fixed log-strike $x \neq 0$. The numerics indicate that for small $t > 0$, as x tends to zero, the asymptotics of option prices and volatility smile explode to infinity. This is in contrast with the standard Heston case [26, section 5].*
- *Since the function Λ is strictly positive and strictly convex on $(u_-, u_+) \setminus \{0\}$ and $u_{\mathfrak{v}_+}(x) \in (u_-, u_+) \setminus \{0\}$ for any $x \neq 0$, the quotient on the right-hand side is well defined.*
- *In a Black–Scholes model we have (see [26, Corollary 3.5])*

$$\mathbb{E}\left(\mathrm{e}^{X_t} - \mathrm{e}^x\right)^+ = (1 - \mathrm{e}^x)^+ + \frac{1}{\sqrt{2\pi x^2}} \exp\left(-\frac{x^2}{2\Sigma^2 t} + \frac{x}{2}\right)(\Sigma^2 t)^{3/2}(1 + \mathcal{O}(t)).$$

Comparing it with Theorem 6.1, we then obtain the higher-order term in the expansion of the implied variance, as t tends to zero:

$$\sigma_t(x)^2 = \frac{x^2}{2\Lambda^*_{\mathfrak{v}_+}(x)} + \frac{x^2 t}{2\Lambda^*_{\mathfrak{v}_+}(x)^2} \log\left(\frac{\mathrm{U}_{\mathfrak{v}_+}(x)\exp(-x/2)(2\Lambda^*_{\mathfrak{v}_+}(x))^{3/2} t}{(\mathfrak{v}_+ - \mathfrak{v}_-)\Lambda(u^*_{\mathfrak{v}_+}(x)) u^*_{\mathfrak{v}_+}(x)^2 \sqrt{\mathfrak{v}_+ \Lambda''(u^*_{\mathfrak{v}_+}(x)) x^2}}\right) + o(t).$$

Proof. The procedure is essentially the same as that of the proof of Theorem 4.11. Applying Lemmas C.2 and C.4, the rescaled cgf of X_t for each t is given by (with the same notation as in (4.1))

$$\begin{aligned}\Lambda_t(u) &:= \Lambda_1\left(t, \frac{u}{t}\right) = t\mathrm{C}\left(t, \frac{u}{t}\right) + t\log\left(\mathrm{M}_{\mathcal{V}} \circ \mathrm{D}\left(t, \frac{u}{t}\right)\right) \\ &= t\mathrm{C}\left(t, \frac{u}{t}\right) + t\log\left(\frac{\mathrm{e}^{\mathfrak{v}_+\mathrm{D}(t,u/t)} - \mathrm{e}^{\mathfrak{v}_-\mathrm{D}(t,u/t)}}{(\mathfrak{v}_+ - \mathfrak{v}_-)\mathrm{D}(t,u/t)}\right) \\ &= \mathfrak{v}_+\Lambda(u) + t\left(\mathrm{C}_0(u) + \mathfrak{v}_+\mathrm{D}_0^0(u) - \log\left((\mathfrak{v}_+ - \mathfrak{v}_-)\Lambda(u)\right)\right) + t\log t + \mathcal{O}\left(t^2\right).\end{aligned} \tag{6.2}$$

For fixed $x > 0$ and small enough $t > 0$, introduce the time-dependent probability measure $\mathbb{Q}_t$ by

$$\frac{\mathrm{d}\mathbb{Q}_t}{\mathrm{d}\mathbb{P}} := \exp\left(\frac{u^*_{\mathfrak{v}_+}(x)X_t - \Lambda_t(u^*_{\mathfrak{v}_+}(x))}{t}\right).$$

Changing the measure, plugging in (6.2), and rearranging terms yield the following expression for the call option price with strike e^x:

$$\begin{aligned}&\mathbb{E}\left(\mathrm{e}^{X_t} - \mathrm{e}^x\right)^+ \\ &= \exp\left(-\frac{\Lambda^*_{\mathfrak{v}_+}(x)}{t}\right)\mathrm{U}_{\mathfrak{v}_+}(x)\frac{t\left(1+\mathcal{O}(t)\right)}{(\mathfrak{v}_+ - \mathfrak{v}_-)\Lambda(u^*_{\mathfrak{v}_+}(x))}\mathbb{E}^{\mathbb{Q}_t}\left[\exp\left(\frac{-u^*_{\mathfrak{v}_+}(x)(X_t - x)}{t}\right)\left(\mathrm{e}^{X_t - x} - 1\right)^+\right].\end{aligned}$$

It is easy to show that, for fixed $t > 0$, under $\mathbb{Q}_t$ the random variable $\left(\frac{X_t - x}{\sqrt{t}}\right)$ converges weakly to a Gaussian distribution. The rest of the proof is similar to that of section D.2, so we omit the details. ∎

We now explain the steepness of the volatility smile in the uncorrelated case $\rho = 0$. Using the at-the-money curvature formula for the implied volatility (in uncorrelated stochastic volatility models) proved by De Marco and Martini [17, Equation (2.9)], we can write, for any $t > 0$,

$$\partial_x^2\sigma(t,x)^2\big|_{x=0} = \frac{2}{t}\left\{\sigma(t,0)\sqrt{2\pi t}\exp\left(\frac{\sigma(t,0)^2 t}{8}\right)p_t(0) - 1\right\}, \tag{6.3}$$

where p_t is the density of the log-price process at time t. In the standard Heston model with initial condition $V_0 = v_0 \in (\mathfrak{v}_-, \mathfrak{v}_+)$, such that $\mathbb{E}(\sqrt{\mathcal{V}}) = \sqrt{v_0}$, the small-time asymptotics of the density reads [30, section 5.3]

$$p_t(x) = \exp\left(-\frac{\Lambda^*_{v_0}(x)}{t}\right)\frac{\mathrm{U}_{v_0}(x)}{\sqrt{2\pi v_0\Lambda''(x)}}t^{-1/2}\left(1 + o(1)\right) \quad \text{for any } x \neq 0,$$

with the function U defined in (6.1). Applying the saddle point method similar to the proof of [26, Theorem 3.1], the small-time asymptotics of the density in a randomized setting, denoted by $\widetilde{p}_t$, has the expression

$$\widetilde{p}_t(x) = \exp\left(-\frac{\Lambda^*_{\mathfrak{v}_+}(x)}{t}\right)\frac{\mathrm{U}_{\mathfrak{v}_+}(x)}{\sqrt{2\pi\mathfrak{v}_+\Lambda''(x)}}\frac{t^{1/2}\left(1 + o(1)\right)}{(\mathfrak{v}_+ - \mathfrak{v}_-)\Lambda(u^*_{\mathfrak{v}_+}(x))}, \quad x \neq 0.$$

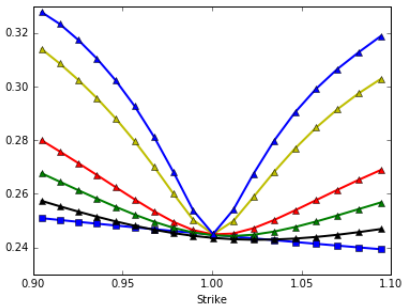

Figure 2. *Uniform randomization with* $(\mathfrak{v}_-, \mathfrak{v}_+) = (0, 0.135)$. *Blue squares represent the implied volatility obtained from the standard Heston model, with maturity* $t = 0.005$. *Blue, yellow, red, green, and black triangles represent the implied volatilities computed from the randomized Heston model by FFT, with the maturities equal to* 0.005, 0.01, 0.05, 0.1, *and* 0.2. *The graph illustrates the increase of steepness in a randomized Heston setting as the maturity tends to zero.*

Remark 6.3. *Note the difference between the powers* $t^{1/2}$ *and* $t^{-1/2}$ *in the expressions for* p_t *and* $\widetilde{p}_t$ *above. Even if, in the bounded support case, the leading-order term is not affected by the randomization, the latter does act at higher order. We leave a precise study of this issue to further research.*

The ratio $p_t(x)/\widetilde{p}_t(x)$ then reads

$$\frac{p_t(x)}{\widetilde{p}_t(x)} = \frac{1}{t}\exp\left(-\frac{\Lambda^*_{v_0}(x) - \Lambda^*_{\mathfrak{v}_+}(x)}{t}\right)\left(\frac{\mathfrak{v}_+}{v_0}\right)^{\frac{1}{2}}\frac{\mathrm{U}_{v_0}(x)}{\mathrm{U}_{\mathfrak{v}_+}(x)}(\mathfrak{v}_+ - \mathfrak{v}_-)\Lambda(u^*_{\mathfrak{v}_+}(x))\,(1+o(1))\,, \quad x \neq 0.$$

It is easy to verify that $\lim_{x\downarrow 0}\mathrm{U}_{v_0}(x) = \lim_{x\downarrow 0}\mathrm{U}_{\mathfrak{v}_+}(x) = 1$ and $\lim_{x\downarrow 0}\Lambda(u^*_{\mathfrak{v}_+}(x)) = 0$. Moreover, for any fixed $x \neq 0$,

$$\partial_v\Lambda^*_v(x) = \partial_v\left[u^*_v(x)x - v\Lambda(u^*_v(x))\right] = \left[x - v\Lambda'(u^*_v(x))\right]\frac{\partial u^*_v(x)}{\partial v} - \Lambda(u^*_v(x)) = -\Lambda(u^*_v(x)) < 0.$$

Combining these results, assume that the density at zero can be approximated by $p_t(x)$ for small enough $x > 0$. Then there exists $t^* > 0$ small enough such that $p_t(x)/\tilde{p}_t(x) < 1$ for all $t \in (0, t^*)$. Plugging it back into (6.3), and noticing that (see section 4.5) $\sigma(t,0) \sim \mathbb{E}[\sqrt{\mathcal{V}}] = \sqrt{v_0} \sim \sigma_t(0, v_0)$ holds as t tends to zero, then the small-time curvature in a uniformly randomized Heston is much larger compared with that of a standard Heston, implying a much steeper smile around the at-the-money. Figure 2 provides some visual help.

Finally, we mention that the tail behavior of the implied volatility in a uniformly randomized Heston model is similar to that of the standard Heston. To see this, notice that the moment explosion property in the standard Heston setting is described in [3, Proposition 3.1]. Specifically, the explosion of the mgf of X_t is equivalent to the explosion of the function D provided in (A.1). Moreover, (2.3) suggests that this is still the case in the uniform randomized setting, since $\mathfrak{m}$ is infinity. Then the similarity of the tail behaviors follows from [45] (see also [9, 13]).

6.2. Noncentral χ-squared distribution. Assume that $\mathcal{V}$ is noncentral χ-squared distributed with $q > 0$ degrees of freedom and noncentrality parameter $\lambda > 0$, so that its mgf reads

$$\mathrm{M}_{\mathcal{V}}(u) = \frac{1}{(1-2u)^{q/2}} \exp\left(\frac{\lambda u}{1-2u}\right) \qquad \text{for all } u \in \mathcal{D}_{\mathcal{V}} = (-\infty, 1/2).$$

Then $\mathfrak{v}_+$ is infinite and $\mathfrak{m} = 1/2$. By Proposition 4.1, the only suitable scale function is $h(t) \equiv \sqrt{t}$, which corresponds exactly to the forward-start Heston model, the asymptotics of which have been studied thoroughly in [39]. Applying (D.3) and L'Hôpital's rule with $\mathrm{M}'_{\mathcal{V}}(u) = \mathrm{M}_{\mathcal{V}}(u)\left(\lambda(1-2u)^{-2} + q(1-2u)^{-1}\right)$ implies that, at the right endpoint $u = \sqrt{2\mathfrak{m}} = 1$, as t tends to zero, the pointwise limit

$$\lim_{t\downarrow 0} \Lambda_{1/2}\left(t, \frac{1}{\sqrt{t}}\right) = \frac{4}{2-\rho\xi} \lim_{s\downarrow 0} \frac{s^2 \mathrm{M}'_{\mathcal{V}}(1/2-s)}{\mathrm{M}_{\mathcal{V}}(1/2-s)} = \frac{\lambda}{2-\rho\xi}$$

can be either finite or infinite. In particular, since $\lambda > 0$, the pointwise limiting rescaled cgf is not continuous at the right boundary of its effective domain. The cgf of $\mathcal{V}$ satisfies Assumption 4.8 with $\omega = 2$. Then Theorem 4.11 implies that we can recover [39, Theorem 4.1]

$$\sigma_t^2(x) = \frac{|x|}{2} t^{-1/2} + \frac{\sqrt{\lambda|x|}}{2} t^{-1/4} + o\left(t^{-1/4}\right), \quad \text{as } t \text{ tends to zero.}$$

6.3. Folded Gaussian distribution. Assume that $\mathcal{V} \overset{(\mathrm{Law})}{=} |\mathcal{N}(0,1)|$. Then the density of $\mathcal{V}$ reads

$$f(v) = \sqrt{\frac{2}{\pi}} \exp\left(-\frac{1}{2}v^2\right) \qquad \text{for all } v \in \mathcal{D}_{\mathcal{V}} = \mathbb{R}_+,$$

which satisfies Assumption 4.4. Simple computations yield $\mathrm{M}_{\mathcal{V}}(z) = 2\exp\left(z^2/2\right)\Phi(z)$ for any $z \in \mathbb{R}$, where Φ denotes the Gaussian cumulative distribution function. Therefore, Lemma C.2 implies that for $\gamma \in (0,1)$,

$$t^{\gamma} \log \mathrm{M}_{\mathcal{V}}\left(\mathrm{D}\left(t, \frac{u}{t^{\gamma}}\right)\right) = \frac{u^4}{8} t^{2-3\gamma} + \frac{\rho\xi u^5}{8} t^{3-4\gamma} - \frac{u^3}{4} t^{2-2\gamma} + \mathcal{O}\left(t^{4-5\gamma}\right) + \mathcal{O}\left(t^{\gamma}\right).$$

If $\gamma = 1$, then $\mathrm{M}_{\mathcal{V}}(x\Lambda(u)) = 2\exp\left(\frac{1}{2}\Lambda^2(u)x^2\right)\Phi(x\Lambda(u))$, and hence

$$t \log \mathrm{M}_{\mathcal{V}}\left(\mathrm{D}\left(t, \frac{u}{t}\right)\right) = \frac{\Lambda^2(u)}{2t} + \mathrm{D}_0^0(u) + \mathcal{O}(t).$$

The limit is therefore nondegenerate if and only if $h(t) = t^{2/3}$, in which case $\Lambda_{2/3}(u) = \frac{1}{8}u^4$ for all $u \in \mathbb{R}$, and Theorem 4.5 implies

$$\lim_{t\downarrow 0} t^{1/3} \sigma_t^2(x) = \frac{(2x)^{2/3}}{3} \quad \text{for all } x \neq 0.$$

6.4. Starting from the ergodic distribution. Remark 2.1 shows that the stationary distribution of a randomized Heston model has the density

$$f_\infty(v) = \frac{a^b}{\Gamma(b)} v^{b-1} \mathrm{e}^{-av} \quad \text{for } v > 0,$$

where $a := \frac{2\kappa}{\xi^2}$ and $b := a\theta$. Assume now that f_∞ is the density of $\mathcal{V}$, so that the cgf of $\mathcal{V}$ is given by $\log \mathrm{M}_\mathcal{V}(u) = -b \log(a-u) + b \log a$, with $u < a = \mathfrak{m}$. Then Assumption 4.8 is satisfied with $\omega = 1$. A direct application of Theorem 4.11 implies that

$$\sigma_t^2(x) = \frac{\xi |x|}{4\sqrt{\kappa t}} + o\left(t^{-1/2}\right) \quad \text{for any } x \neq 0.$$

6.5. Other distributions. Table 1 (a more refined version of the table in section 1) presents some common continuous distributions for the initial variance, together with the corresponding parameters $\mathfrak{v}_+, \mathfrak{m}, l_2$. In each case, we indicate (up to a constant multiplier) the short-time behavior of the smile.

Table 1
Some continuous distributions with support in $\mathbb{R}_+$.

Name	$\mathfrak{v}_+$	$\mathfrak{m}$	l_2	Behavior of $\sigma_t^2(x)$ $(x \neq 0)$	Reference
Beta	1	∞		$x^2/\Lambda_1^*(x)$	Equation (4.3)
Exponential(λ)	∞	$\lambda < \infty$	1	$\lvert x\rvert t^{-1/2}$	Theorem 4.11
χ-squared	∞	1/2	1	$\lvert x\rvert t^{-1/2}$	Theorem 4.11
Rayleigh	∞	∞	2	$x^{2/3} t^{-1/3}$	Theorem 4.5
Weibull ($k > 1$)	∞	∞	k	$(x^2/t)^{1/(1+k)}$	Theorem 4.5

6.6. Numerics. We present numerical results for the implied volatility surface for three types of initial randomization: uniform ($\mathfrak{v}_+ < \infty$), exponential ($\mathfrak{m} < \mathfrak{v}_+ = \infty$), and folded-Gaussian ($\mathfrak{m} = \mathfrak{v}_+ = \infty$). To generate these surfaces, we apply fast Fourier transform (FFT) methods [14] to derive a matrix of option prices, and then we compute the corresponding implied volatilities using a root-finding algorithm. The Heston parameters are given by $(\kappa, \theta, \xi, V_0, \rho) = (2.1, 0.05, 0.1, 0.06, -0.6)$, which corresponds to a realistic data set calibrated on the S&P options data. In view of Theorem 4.20, parameters of $\mathcal{V}$ are chosen to satisfy $\mathbb{E}(\sqrt{\mathcal{V}}) = \sqrt{V_0}$, so that results of standard and randomized Heston models can be compared.

The numerics show that the randomized Heston model provides a much steeper short-time volatility smile compared with the standard Heston model, but this difference tends to fade away as maturity increases. In the uniform case, Figure 3 and (4.3) may seem contradictory at first, since the former indicates steepness and the latter excludes explosion. There is no issue here, and in fact this suggests that even though there is no proper explosion, it is still possible to generate steep short-time volatility smiles in a randomized setting. In Figure 4, we show the impact of a random distribution following a folded Gaussian on the implied volatility smile, leaving the Heston parameters unchanged. In Figure 5 we test higher-order terms in a Gamma randomization scheme while the Heston parameters remain unchanged.

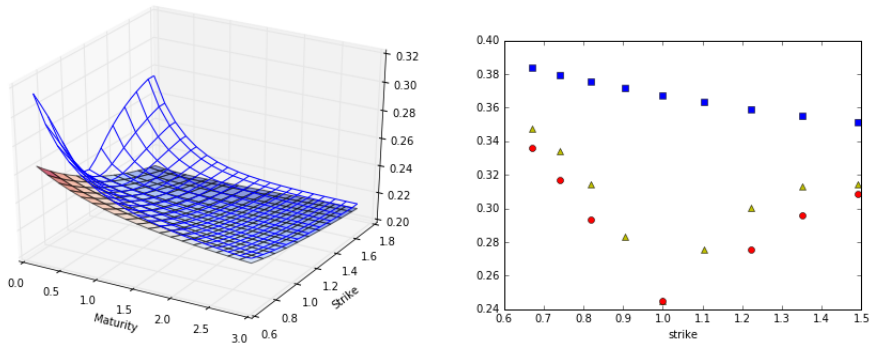

Figure 3. *Uniform randomization with* $(\mathfrak{v}_-, \mathfrak{v}_+) = (0, 0.135)$. *Time to maturity is represented in years. Left: volatility surfaces of randomized and standard Heston calculated with the FFT method. Right: triangles, squares, and circles represent implied volatility by FFT, leading-, and second-order asymptotics. Time to maturity is* $t = 1/24$. *Higher-order terms are obtained by inverting the asymptotic formula in Theorem 6.1 (see also Remark 6.2).*

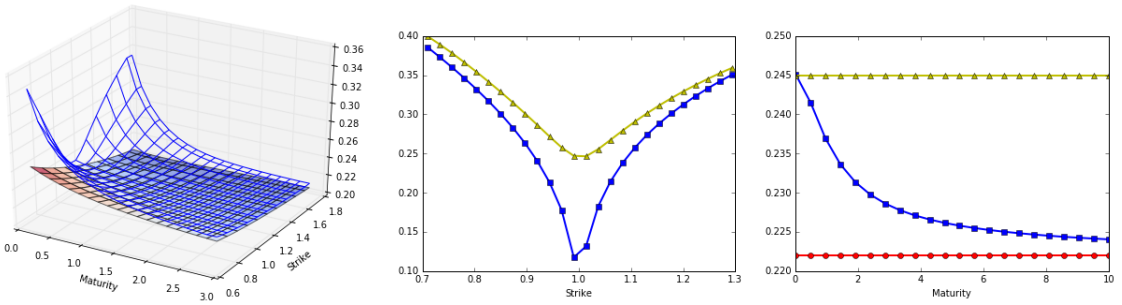

Figure 4. $\mathcal{V} \overset{(Law)}{=}$ *folded-Gaussian. Left: implied volatility surfaces of folded-Gaussian randomization and standard Heston, calculated using FFT. Middle: implied volatility by FFT (triangles) and the leading order (squares) in Theorem 4.5,* $t = 1/24$. *Right: triangles, squares, and circles represent* $\sqrt{V_0}$, *at-the-money implied volatility* $\sigma_t(0)$ *by FFT, and large-time limit. The parameter* l_1 *in Assumption 4.4 is* 63.46.

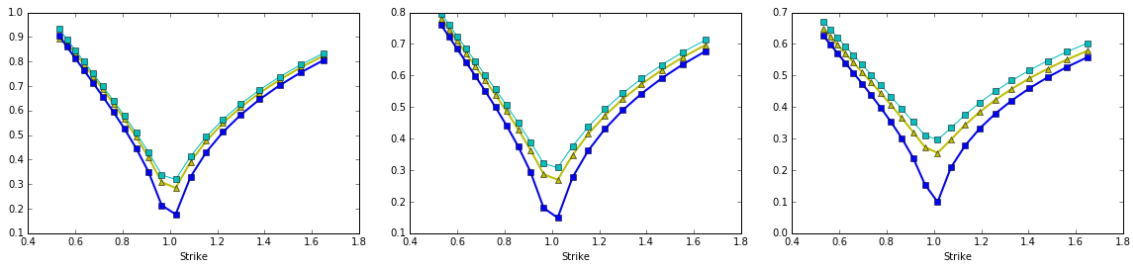

Figure 5. $\mathcal{V} \overset{(Law)}{=} \Gamma(\alpha, \beta)$ *with* $(\alpha, \beta) = (0.4, 3.868)$. *Here we preset* α *and calculate* β *using Theorem 4.20. Blue and cyan squares are first- and second-order asymptotics, and yellow triangles are true smiles by FFT. From left to right, maturities are one week, two weeks, and one month.*

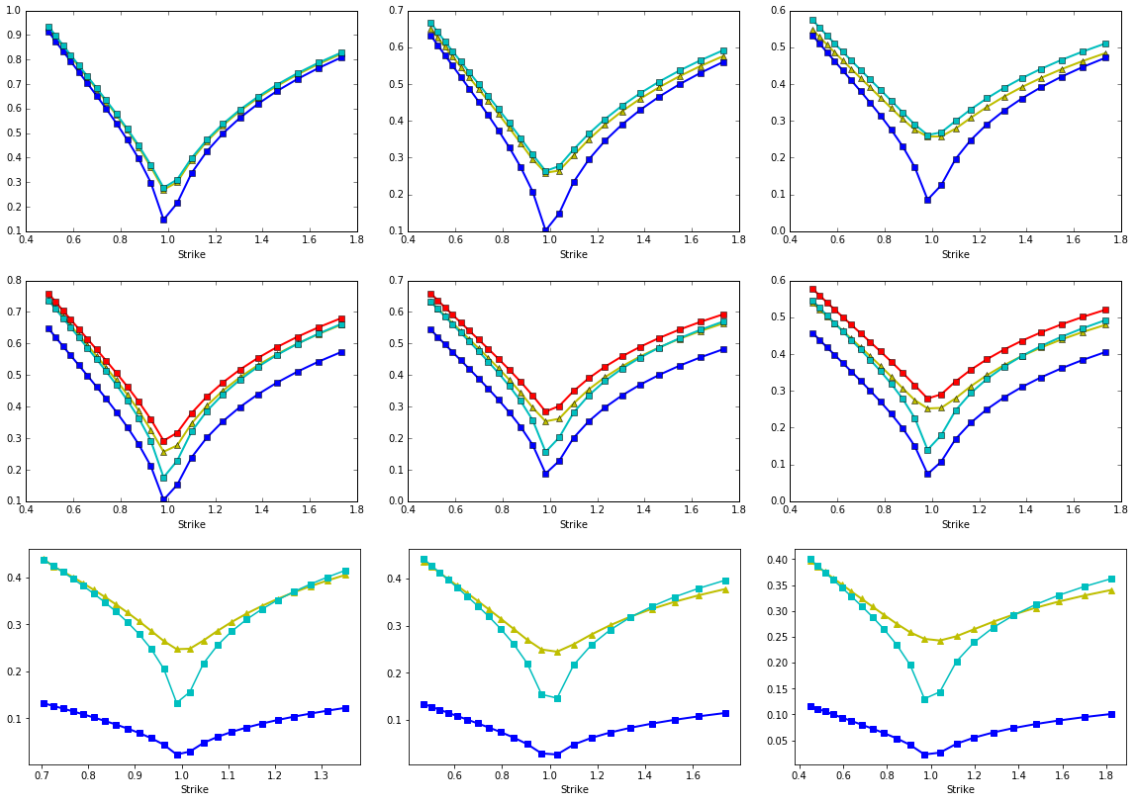

Figure 6. *Numerical examples for the dynamic pricing framework. We price the option at* $\breve{t} = 1/12$ *in three different randomization schemes: Gamma (*$\Gamma(0.4, 3.868)$*, top), noncentral* χ*-squared (*$0.07\chi^2(0.23, 1.25)$*, middle), and folded-Gaussian (*$l_2 = 2$*,* $l_1 = 63.46$*, bottom). Time to maturity* τ *is one week, one month, two months (left to right). Blue and cyan squares are first- and second-order asymptotics, red squares (in the second row) are third-order asymptotics, and yellow triangles are true implied volatilities computed by FFT.*

In Figure 6 we illustrate the results in section 5. We price the option in three different randomization schemes after one month ($\breve{t} = 1/12$) into the life of the contract. To compare different schemes, we again match the parameters of $\mathcal{V}$ (at time zero) with different distributions according to Theorem 4.20. We see that the higher-order term in Theorem 4.11 is quite accurate even for relatively large time to maturity. Not surprisingly (especially in the folded-Gaussian case) the leading order is insufficient, and higher orders are needed for reliable approximations.

6.7. USD/JPY FX options. We test the calibration accuracy of the randomized Heston model using the USD/JPY FX market (ask) prices on January 20th, 2017. In the FX market the implied volatility still has the small-time explosion feature: Figure 7 shows that the volatility smile generated by a standard Heston model is too flat compared with the market data with small maturities. This finding agrees with the existing literature. For instance, in [42] the authors fixed κ and v_0 and calibrated the remaining 3 parameters (θ, ξ, ρ) in a standard Heston environment to the EUR/USD market data. They selected maturities ranging from one week to two years, then calibrated the Heston model for each fixed maturity. Even with

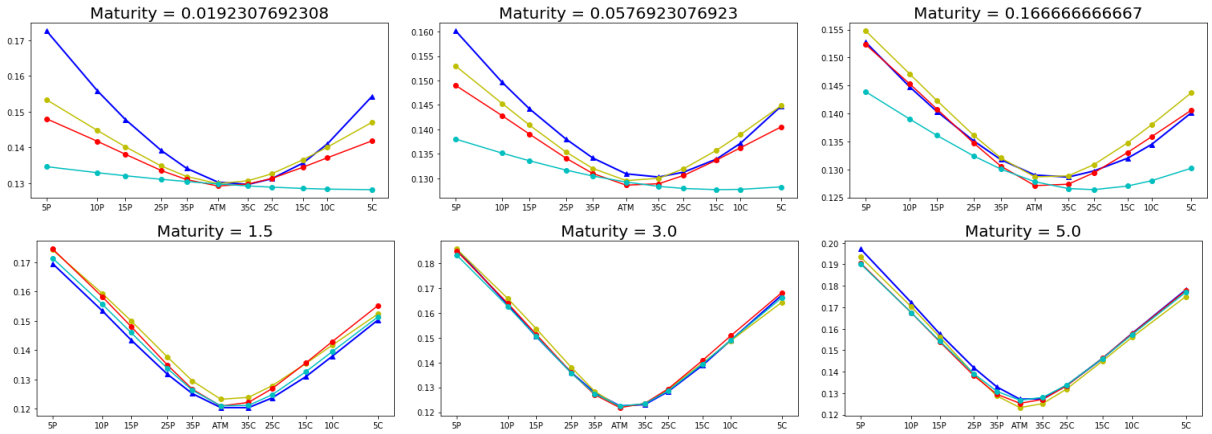

Figure 7. *Calibration results of the randomized Heston model with Gamma (yellow) and uniform (red) randomizations, compared to the standard Heston model (cyan).*

this "slice-by-slice" calibration procedure, they observed poor fit of Heston to the market data for small maturities. Unsurprisingly, they commented that time-dependent parameters, or "stochastic volatility plus jumps," as appeared in [5, 6], are needed to improve the calibration accuracy. We use the same initial guess for both the standard and the randomized Heston models, then calibrate the parameter sets using the market data. The results are presented in Figure 7 and Table 2. Both randomization schemes show a substantial improvement over the standard Heston model.

Table 2

The root-mean-square deviation (RMSD) of standard and randomized Heston models ($\times 10^{-3}$). Small maturities are those less than one month; the total RMSD is calculated over all maturities including extrapolations up to seven years.

Model	Small maturities	Less than one year	Total
Standard Heston	11.91	8.22	7.34
Gamma randomization	5.86	5.02	5.32
Uniform randomization	6.86	5.13	5.51

Appendix A. Notation from the Heston model. In the Heston model, the log stock price satisfies the SDE (2.1), where the initial distribution $\mathcal{V}$ is a Dirac mass at some point $v_0 > 0$. As proved in [1], the mgf (2.2) admits the closed-form representation $\mathrm{M}(t,u) = \exp\big(\mathrm{C}(t,u) + \mathrm{D}(t,u)v_0\big)$ for any $u \in \mathcal{D}_{\mathrm{M}}^t$, where

$$\text{(A.1)} \qquad \begin{cases} \mathrm{C}(t,u) := \dfrac{\kappa\theta}{\xi^2}\left[(\kappa - \rho\xi u - d(u))t - 2\log\left(\dfrac{1-g(u)\mathrm{e}^{-d(u)t}}{1-g(u)}\right)\right], \\ \mathrm{D}(t,u) := \dfrac{\kappa - \rho\xi u - d(u)}{\xi^2}\dfrac{1-\exp\left(-d(u)t\right)}{1-g(u)\exp\left(-d(u)t\right)}, \\ d(u) := \big((\kappa-\rho\xi u)^2 + \xi^2 u(1-u)\big)^{1/2} \qquad \text{and} \qquad g(u) := \dfrac{\kappa-\rho\xi u - d(u)}{\kappa - \rho\xi u + d(u)}. \end{cases}$$

In the proof of [26, Lemma 6.1], the authors showed that the functions d and g have the following behavior as t tends to zero:

$$d\left(\frac{u}{t}\right) = \mathtt{i}\frac{d_0 u}{t} + d_1 + \mathcal{O}(t) \qquad \text{and} \qquad g\left(\frac{u}{t}\right) = g_0 - \mathtt{i}\frac{g_1}{u}t + \mathcal{O}(t^2), \tag{A.2}$$

with $d_0 := \xi\overline{\rho}\,\mathrm{sgn}(u)$, $d_1 := \mathtt{i}\frac{2\kappa\rho-\xi}{2\overline{\rho}}\mathrm{sgn}(u)$, $g_0 := \frac{\mathtt{i}\rho-\overline{\rho}\mathrm{sgn}(u)}{\mathtt{i}\rho+\overline{\rho}\,\mathrm{sgn}(u)}$ and $g_1 := \frac{(2\kappa-\rho\xi)\mathrm{sgn}(u)}{\xi\overline{\rho}(\overline{\rho}+\mathtt{i}\rho\,\mathrm{sgn}(u))^2}$. The pointwise limit of the (rescaled) cgf of X_t then reads

$$\lim_{t\downarrow 0} t\log \mathrm{M}\left(t, \frac{u}{t}\right) = \Lambda(u)v_0 \qquad \text{for any } u \in (u_-, u_+),$$

where u_-, u_+, and Λ are introduced in (4.2). From [26, section 2], the function Λ is well defined, smooth, and strictly convex on (u_-, u_+), and is infinite elsewhere.

Appendix B. Reminder on large deviations and regular variations.

B.1. Large deviations and the Gärtner–Ellis theorem. In this appendix, we briefly recall the main definitions and results from large deviations theory, which we need in this paper. For full details, the interested reader is advised to look at the excellent monograph by Dembo and Zeitouni [19]. Let $(Y_n)_{n\geq 0}$ denote a sequence of real-valued random variables. A map $I : \mathbb{R} \to \mathbb{R}_+$ is said to be a good rate function if it is lower semicontinuous and if the set $\{y : I(y) \leq \alpha\}$ is compact in $\mathbb{R}$ for each $\alpha \geq 0$.

Definition B.1. *Let $h : \mathbb{R} \to \mathbb{R}_+$ be a continuous function that tends to zero at infinity. The sequence $(Y_n)_{n\geq 0}$ satisfies a large deviations principle as n tends to infinity with speed $h(n)$ and rate function I (in our notation, $Y \sim \mathrm{LDP}_\infty(h(n), I)$) if for each Borel measurable set $\mathcal{S} \subset \mathbb{R}$ the following inequalities hold:*

$$-\inf_{y\in\mathcal{S}^o} I(y) \leq \liminf_{n\uparrow\infty} h(n)\log\mathbb{P}(Y_n \in \mathcal{S}) \leq \limsup_{n\uparrow\infty} h(n)\log\mathbb{P}(Y_n \in \mathcal{S}) \leq -\inf_{y\in\overline{\mathcal{S}}} I(y).$$

Now let Λ_h be the pointwise limit—whenever the limit exists—of the rescaled cgf of Y: $\Lambda_h(u) := \lim_{n\uparrow\infty} h(n)\log\mathbb{E}\big[\exp(uY_n/h(n))\big]$, and denote by $\mathcal{D}_\Lambda := \{u \in \mathbb{R} : |\Lambda_h(u)| < \infty\}$ its effective domain. Then Λ_h is said to be essentially smooth if the interior $\mathcal{D}_\Lambda^o$ is nonempty, Λ_h is differentiable on $\mathcal{D}_\Lambda^o$, and $\lim_{u\to u_0} |\Lambda_h'(u)| = \infty$ for any $u_0 \in \partial\mathcal{D}_\Lambda$. Finally, for any $y \in \mathbb{R}$, define $\Lambda_h^*(y) := \sup_{u\in\mathcal{D}_\Lambda}\{uy - \Lambda_h(u)\}$ to be the convex conjugate of function Λ_h.

Theorem B.2 (Gärtner–Ellis theorem, Theorem 2.3.6 in [19]). *If the function Λ_h is lower semicontinuous on $\mathcal{D}_\Lambda$ and essentially smooth, and $0 \in \mathcal{D}_\Lambda^o$, then $(Y_n)_{n\geq 0} \sim \mathrm{LDP}_\infty(h(n), \Lambda_h^*)$.*

B.2. Regular variations. We recall here some notions on regular variations, following the monograph [10].

Definition B.3. *Let $\mathfrak{a} > 0$. A function $f : (\mathfrak{a}, \infty) \to \mathbb{R}_+^*$ is said to be regularly varying with index $l \in \mathbb{R}$ (and we write $f \in \mathcal{R}_l$) if $\lim_{x\uparrow\infty} f(\lambda x)/f(x) = \lambda^l$ for any $\lambda > 0$. When $l = 0$, the function f is called slowly varying.*

Lemma B.4 (Bingham's lemma, Theorem 4.12.10 in [10]). *Let f be a regularly varying function with index $l > 0$; then, as x tends to infinity, the asymptotic equivalence $-\log\int_x^\infty \mathrm{e}^{-f(y)}\mathrm{d}y \sim f(x)$ holds.*

Let Y be a random variable supported on $[0,\infty)$ with a smooth density f. The following lemma ensures that its mgf has unbounded support.

Lemma B.5. *If there exists $l>1$ such that $|\log f|\in\mathcal{R}_l$, then* $\sup\{u\in\mathbb{R}:\mathbb{E}(\mathrm{e}^{uY})<\infty\}=+\infty$.

Proof. Karamata's characterization theorem [10, Theorem 1.4.1] implies that $|\log f(v)|=v^l g(v)$ for any $v>0$, where the function g is slowly varying, and Karamata's representation theorem [10, Theorem 1.3.1] provides the following expression:

$$g(v)=\mathrm{c}(v)\exp\left(\int_a^v \varepsilon(y)\frac{\mathrm{d}y}{y}\right),$$

where the functions c and ε satisfy $\lim_{v\uparrow\infty}\mathrm{c}(v)=c>0$, $\lim_{v\uparrow\infty}\varepsilon(v)=0$, and a is a fixed positive number. Then there exists $v_1\geq a$ such that $\mathrm{c}(v)>c/2$ for all $v\geq v_1$. Additionally, for any small enough fixed ε_0 satisfying that $l>1+\varepsilon_0$, there exists $v_2\geq a$ such that $\int_{v_2}^v\varepsilon(y)\mathrm{d}y/y>-\varepsilon_0\log(v/v_2)$ for any $v\geq v_2$. Denote $d:=\exp\big(\int_a^{v_2}\varepsilon(y)\frac{\mathrm{d}y}{y}\big)$. Then for any $v>\max(v_1,v_2)$, and any $u>0$,

$$u-\mathrm{c}(v)\exp\left(\int_a^v\varepsilon(y)\frac{\mathrm{d}y}{y}\right)v^{l-1}<u-\frac{cd}{2}\exp\left(\int_{v_2}^v\varepsilon(y)\frac{\mathrm{d}y}{y}\right)v^{l-1}<u-\frac{cd}{2}v_2^{\varepsilon_0}v^{l-1-\varepsilon_0}.$$

Thus there exists v_3 large enough so that $u-\frac{1}{2}cdv_2^{\varepsilon_0}v^{l-1-\varepsilon_0}<-1$ for $v\geq v_3$. With $v^*:=\max(v_1,v_2,v_3)$,

$$\mathbb{E}\left(\mathrm{e}^{uY}\right)=\int_0^{v^*}\mathrm{e}^{uv}f(v)\mathrm{d}v+\int_{v^*}^{\infty}\mathrm{e}^{v\left(u-v^{l-1}g(v)\right)}\mathrm{d}v<\int_0^{v^*}\mathrm{e}^{uv}f(v)\mathrm{d}v+\int_{v^*}^{\infty}\mathrm{e}^{-v}\mathrm{d}v<\infty.$$ ∎

Appendix C. Preliminary computations.

In view of (2.3), short-time asymptotic expansions of the functions C and D are necessary in order to derive the pointwise limit of the rescaled cgf of $(X_t)_{t\geq0}$. In this appendix we provide these expansions.

C.1. Components of the mgf.

We start by investigating the short-time behavior of the function $\mathrm{D}(t,u/h(t))$. For any $\beta\in\mathbb{R}$, define the function $\mathrm{D}_0^\beta:(u_-,u_+)\to\mathbb{R}$ by

(C.1)
$$\begin{aligned}\mathrm{D}_0^\beta(u):=&\frac{1-\mathrm{e}^{-\mathtt{i}d_0u}}{\xi^2(1-g_0\mathrm{e}^{-\mathtt{i}d_0u})}\left[(\rho\xi+\mathtt{i}d_0)\beta u+\kappa-d_1\right]+\frac{\mathtt{i}g_1(\rho\xi+\mathtt{i}d_0)}{\xi^2}\frac{1-\mathrm{e}^{-\mathtt{i}d_0u}}{(1-g_0\mathrm{e}^{-\mathtt{i}d_0u})^2}\mathrm{e}^{-\mathtt{i}d_0u}\\&-\frac{(\rho\xi+\mathtt{i}d_0)u}{\xi^2}\frac{d_1-\mathtt{i}d_0u\beta}{(1-g_0\mathrm{e}^{-\mathtt{i}d_0u})^2}(1-g_0)\,\mathrm{e}^{-\mathtt{i}d_0u},\end{aligned}$$

where the functions d_0,d_1,g_0,g_1 are defined below (A.2).

Remark C.1. *The function D_0^β is well defined; to see this, we only need to check that the β terms sum up to a real number, and the rest follows from* [26, Remark 3.2]. *The first term in* (C.1) *reads*

$$\frac{1-\mathrm{e}^{-\mathtt{i}d_0u}}{\xi^2(1-g_0\mathrm{e}^{-\mathtt{i}d_0u})}(\rho\xi+\mathtt{i}d_0)\beta u=-\beta\Lambda(u),$$

which is a real number, and the sum of the remaining terms with β reads (taking out the prefactor $\mathtt{i}d_0u\beta$)

$$\frac{(\rho\xi+\mathtt{i}d_0)u\mathrm{e}^{-\mathtt{i}d_0u}(1-g_0)}{\xi^2(1-g_0\exp(-\mathtt{i}d_0u))^2}=\frac{(g_0-1)\mathrm{e}^{-\mathtt{i}d_0u}\Lambda(u)}{(1-g_0\mathrm{e}^{-\mathtt{i}d_0u})(1-\mathrm{e}^{-\mathtt{i}d_0u})}=\frac{\mathtt{i}\overline{\rho}\,\mathrm{sgn}(u)\Lambda(u)}{\rho\cos(d_0u)+\overline{\rho}\,\mathrm{sgn}(u)\sin(d_0u)-\rho},$$

which is purely imaginary, so that the whole term is a real number.

The following lemma makes the effective domain of D_0^β precise and shows that it arises as the second order of the short-time expansion of a rescaled version of the function D in (A.1).

Lemma C.2. *Let $\beta\in\mathbb{R}$. As t tends to zero, the map $t\mapsto \mathrm{D}\left(t,u/h(t)\right)$ behaves as*

$$\mathrm{D}\left(t,\frac{u}{h(t)}\right)=\begin{cases}0, & u=0, \quad \text{for any function } h,\\ \text{undefined}, & u\neq0, \quad \text{if } h(t)=o(t),\\ t^{-1}\Lambda(u)+\mathrm{D}_0^\beta(u)+o(1), & u\in(u_-,u_+), \quad \text{if } h(t)=t+\beta t^2+o(t^2),\\ \dfrac{u^2t}{2h^2(t)}\left[1-\dfrac{h(t)}{u}+\dfrac{\rho\xi ut}{2h(t)}+\mathcal{O}\left(t+h^2(t)+\dfrac{t^2}{h^2(t)}\right)\right], & u\in\mathbb{R}, \quad \text{if } t=o(h(t)).\end{cases}$$

Remark C.3.

(i) *If $h(t)=t+o(t)$ without further information on higher-order terms (third case in the lemma), then only the leading order is available: $\mathrm{D}\big(t,u/h(t)\big)=t^{-1}\Lambda(u)(1+o(1))$.*
(ii) *As in Remark 4.2(ii), one can consider $h(t)=ct+\beta t^2+o(t^2)$, but by dilation, setting $c=1$ is inconsequential.*
(iii) *When $h(t)=t^{1/2}$, $\mathrm{D}\big(t,\frac{u}{h(t)}\big)=\frac{1}{2}u^2+\frac{1}{4}\left(\rho\xi u^2-2\right)ut^{1/2}+\mathcal{O}(t)$, which is consistent with* [39, Lemma 6.2].

The function $\mathrm{C}_0:(u_-,u_+)\to\mathbb{R}$ defined as

$$\mathrm{C}_0(u):=-\frac{\kappa\theta}{\xi^2}\left[(\rho\xi+\mathtt{i}d_0)u+2\log\left(\frac{1-g_0\exp(-\mathtt{i}d_0u)}{1-g_0}\right)\right] \tag{C.2}$$

is clearly real-valued [26, Remark 6.2] and determines the asymptotic behavior of the function C as follows.

Lemma C.4. *The map $t\mapsto \mathrm{C}\left(t,u/h(t)\right)$ has the following asymptotic behavior as t tends to zero:*

$$\mathrm{C}\left(t,\frac{u}{h(t)}\right)=\begin{cases}\text{undefined}, & u\neq0, \quad h(t)=o(t),\\ \mathrm{C}_0(u)+\mathcal{O}(t), & u\in(u_-,u_+), \quad h(t)=t+\mathcal{O}(t^2),\\ \mathcal{O}\left(th(t)+h^3(t)\right)+\dfrac{\kappa\theta u^2}{4}\left(\dfrac{t}{h(t)}\right)^2\left[1+\mathcal{O}\left(h(t)+\dfrac{t}{h(t)}\right)\right], & u\in\mathbb{R}, \quad t=o(h(t)).\end{cases}$$

Proof of Lemma C.2. Obviously $\mathrm{D}(t,0)\equiv 0$, so we assume from now on that $u\neq 0$. From (A.2), we have

$$d\left(\frac{u}{h(t)}\right)=\mathtt{i}\frac{d_0u}{h(t)}+d_1+\mathcal{O}(h(t)) \qquad \text{and} \qquad g\left(\frac{u}{h(t)}\right)=g_0-\mathtt{i}\frac{g_1}{u}h(t)+\mathcal{O}\left(h^2(t)\right). \tag{C.3}$$

Plugging these back into the expression of the function D in (A.1), we obtain

$$\mathrm{D}\left(t,\frac{u}{h(t)}\right)=\left[\frac{\kappa-d_1-\frac{\rho\xi u+\mathtt{i}d_0u}{h(t)}+\mathcal{O}(h(t))}{\xi^2}\right]\left[\frac{1-\exp\left\{-\frac{\mathtt{i}ud_0t}{h(t)}-d_1t+\mathcal{O}(th(t))\right\}}{1-\left[g_0-\mathtt{i}\frac{g_1}{u}h(t)+\mathcal{O}(h^2(t))\right]\mathrm{e}^{-\frac{\mathtt{i}ud_0t}{h(t)}-d_1t+\mathcal{O}(th(t))}}\right]. \tag{C.4}$$

If $h(t)=o(t)$, d_0 is a real number, and d_1 is purely imaginary, then as $t/h(t)$ goes to infinity the term $\exp(-\mathtt{i}ud_0t/h(t)-d_1t)$ oscillates on the unit circle in the complex plane; thus no asymptotic can be derived.

Assume now that $h(t)=t+\beta t^2+o(t^2)$. Then $th^{-1}(t)=1-\beta t+o(t)$, and (C.4) yields

$$\begin{aligned}
&\mathrm{D}\left(t,\frac{u}{h(t)}\right)=\frac{1}{\xi^2}\left[-\frac{(\rho\xi+\mathtt{i}d_0)u}{h(t)}+(\kappa-d_1)+\mathcal{O}(h(t))\right]\\
&\left[\frac{1-\exp(-\mathtt{i}d_0ut/h(t)-d_1t+\mathcal{O}(th(t)))}{1-(g_0-\mathtt{i}tg_1/u+\mathcal{O}(t^2))\exp(-\mathtt{i}d_0ut/h(t)-d_1t+\mathcal{O}(th(t)))}\right]\\
&=\frac{1}{\xi^2}\left(-\frac{(\rho\xi+\mathtt{i}d_0)u}{t}(1-\beta t+o(t))+(\kappa-d_1)+\mathcal{O}(t)\right)\left(1-\mathrm{e}^{-\mathtt{i}d_0u}\left(1-d_1t+\mathcal{O}(t^2)\right)(1+\mathtt{i}\beta d_0ut+o(t))\right)\\
&\frac{1}{1-g_0\mathrm{e}^{-\mathtt{i}d_0u}}\left(1+\frac{(-\mathtt{i}g_1/u+g_0(\mathtt{i}d_0u\beta-d_1))\mathrm{e}^{-\mathtt{i}d_0u}}{1-g_0\mathrm{e}^{-\mathtt{i}d_0u}}t+o(t)\right)\\
&=\frac{\mathrm{e}^{-\mathtt{i}d_0u}-1}{\xi^2t}\frac{(\rho\xi+\mathtt{i}d_0)u}{1-g_0\mathrm{e}^{-\mathtt{i}d_0u}}+\frac{1-\mathrm{e}^{-\mathtt{i}d_0u}}{\xi^2(1-g_0\mathrm{e}^{-\mathtt{i}d_0u})}((\rho\xi+\mathtt{i}d_0)\beta u+\kappa-d_1)-\frac{(\rho\xi+\mathtt{i}d_0)u}{\xi^2}\frac{(d_1-\mathtt{i}\beta d_0u)\mathrm{e}^{-\mathtt{i}d_0u}}{1-g_0\mathrm{e}^{-\mathtt{i}d_0u}}\\
&+\frac{(\rho\xi+\mathtt{i}d_0)(\mathtt{i}g_1-g_0u(\mathtt{i}\beta d_0u-d_1))(1-\mathrm{e}^{-\mathtt{i}d_0u})}{\xi^2(1-g_0\mathrm{e}^{-\mathtt{i}d_0u})^2}\mathrm{e}^{-\mathtt{i}d_0u}+o(1)\\
&=\frac{\Lambda(u)}{t}+\mathrm{D}_0^{\beta}(u)+o(1).
\end{aligned}$$

The form of the effective domain is straightforward from these expressions.

If $h(t)=t+o(t)$ without further information on higher-order terms, then $t/h(t)=1+o(1)$. Following the same procedure as above, then only the leading order can be derived, i.e., $\mathrm{D}(t,u/h(t))=t^{-1}\Lambda(u)[1+o(1)]$.

Finally in the case $t=o(h(t))$,

$$\left[1-\left(g_0-\frac{\mathtt{i}g_1}{u}h(t)+\mathcal{O}(h^2(t))\right)\mathrm{e}^{-\frac{\mathtt{i}d_0ut}{h(t)}-d_1t+\mathcal{O}(th(t))}\right]^{-1}=\frac{1-\frac{\mathtt{i}g_1h(t)}{u(1-g_0)}-\frac{\mathtt{i}d_0g_0ut}{(1-g_0)h(t)}+\mathcal{O}\left(t+h^2(t)+\frac{t^2}{h^2(t)}\right)}{1-g_0},$$

$$1-\exp\left(\frac{-\mathtt{i}d_0ut}{h(t)}-d_1t+\mathcal{O}(th(t))\right)=\frac{\mathtt{i}d_0ut}{h(t)}+d_1t+\frac{d_0^2u^2t^2}{2h^2(t)}+\mathcal{O}\left(\frac{t^2}{h(t)}\right)+\mathcal{O}(th(t)).$$

Plugging these results into (C.4) yields

$$
\begin{aligned}
&\mathrm{D}\left(t,\frac{u}{h(t)}\right)\\
&=\frac{1}{\xi^2(1-g_0)}\left[-\frac{(\rho\xi+\mathtt{i}d_0)u}{h(t)}+(\kappa-d_1)+\mathcal{O}(h(t))\right]\left[\frac{\mathtt{i}d_0ut}{h(t)}+d_1t+\frac{d_0^2u^2t^2}{2h^2(t)}+\mathcal{O}\left(\frac{t^2}{h(t)}+th(t)\right)\right]\\
&\quad\left[1-\frac{\mathtt{i}g_1h(t)}{u(1-g_0)}-\frac{\mathtt{i}d_0g_0ut}{(1-g_0)h(t)}+\mathcal{O}\left(t+h^2(t)+\frac{t^2}{h^2(t)}\right)\right]\\
&=\frac{1}{\xi^2(1-g_0)}\left[\frac{(d_0-\mathtt{i}\rho\xi)d_0u^2t}{h^2(t)}+\frac{[\mathtt{i}d_0u(\kappa-d_1)-d_1u(\rho\xi+\mathtt{i}d_0)]t}{h(t)}-\frac{d_0^2u^3(\rho\xi+\mathtt{i}d_0)t^2}{2h^3(t)}+\mathcal{O}\left(t+\frac{t^2}{h^2(t)}\right)\right]\\
&\quad\left[1-\frac{\mathtt{i}g_1h(t)}{u(1-g_0)}-\frac{\mathtt{i}d_0g_0ut}{(1-g_0)h(t)}+\mathcal{O}\left(t+h^2(t)+\frac{t^2}{h^2(t)}\right)\right]\\
&=\frac{u^2t}{2h^2(t)}\left[1-\frac{h(t)}{u}+\frac{\rho\xi ut}{2h(t)}+\mathcal{O}\left(\frac{t^2}{h^2(t)}+h^2(t)+t\right)\right],
\end{aligned}
$$

where we used the identity

$$
\frac{(d_0-\mathtt{i}\rho\xi)d_0}{(1-g_0)\xi^2}=\frac{(\xi\overline{\rho}\mathrm{sgn}(u)-\mathtt{i}\rho\xi)\xi\overline{\rho}\mathrm{sgn}(u)}{\xi^2\left(1-\frac{\mathtt{i}\rho-\overline{\rho}\mathrm{sgn}(u)}{\mathtt{i}\rho+\overline{\rho}\mathrm{sgn}(u)}\right)}=\frac{1}{2}.
$$

■

Proof of Lemma C.4. Assume that $u\neq 0$. Expanding $d(u/h(t))$ and $g(u/h(t))$ to the third order,

$$
\begin{aligned}
d\left(\frac{u}{h(t)}\right)&=\mathtt{i}\frac{d_0u}{h(t)}+d_1-\mathtt{i}d_2h(t)+\mathcal{O}\left(h^2(t)\right),\\
g\left(\frac{u}{h(t)}\right)&=g_0-\mathtt{i}\frac{g_1}{u}h(t)-\mathtt{i}\frac{g_2}{u^2}h^2(t)+\mathcal{O}\left(h^3(t)\right),
\end{aligned}
\tag{C.5}
$$

where $d_2:=(\kappa^2-d_1^2)/(2d_0u)$ and $g_2:=[(\kappa^2-d_1^2)\rho\xi/d_0+(\kappa-d_1)(\rho\xi-\mathtt{i}d_0)g_1](\rho\xi-\mathtt{i}d_0)^{-2}$. Combining these expansions with (C.3) implies

(C.6)

$$
\begin{aligned}
&\mathrm{C}\left(t,\frac{u}{h(t)}\right)\\
&=-\frac{2\kappa\theta}{\xi^2}\log\left(\frac{1-\left(g_0-\mathtt{i}g_1h(t)/u-\mathtt{i}g_2h^2(t)/u^2+\mathcal{O}(h^3(t))\right)\mathrm{e}^{-\mathtt{i}d_0ut/h(t)-d_1t+\mathtt{i}d_2th(t)+\mathcal{O}\left(th^2(t)\right)}}{1-g_0+\mathtt{i}g_1h(t)/u+\mathtt{i}g_2h^2(t)/u^2+\mathcal{O}\left(h^3(t)\right)}\right)\\
&\quad+\frac{\kappa\theta}{\xi^2}\left[(\kappa-d_1)\,t-\frac{(\rho\xi+\mathtt{i}d_0)ut}{h(t)}+\mathcal{O}\left(th(t)\right)\right].
\end{aligned}
$$

If $h(t)=o(t)$, no short-time asymptotics can be derived since $t/h(t)$ tends to infinity. For the proof of the case where $h(t)=t+\mathcal{O}(t^2)$ we refer the reader to [26, Lemma 6.1]. Assume

now that $t = o(h(t))$. Then the following asymptotic expansions hold:

$$\left(1-g_0+\frac{\mathtt{i}h(t)g_1}{u}+\frac{\mathtt{i}h^2(t)g_2}{u^2}+\mathcal{O}\left(h^3(t)\right)\right)^{-1}=\frac{1}{1-g_0}\left(1-\frac{\mathtt{i}g_1h(t)}{u(1-g_0)}-\frac{g_3h^2(t)}{u^2(1-g_0)^2}+\mathcal{O}\left(h^3(t)\right)\right),$$
$$\exp\left(-\frac{\mathtt{i}d_0ut}{h(t)}-d_1t+\mathtt{i}d_2th(t)+\mathcal{O}\left(th^2(t)\right)\right)=1-\frac{\mathtt{i}d_0ut}{h(t)}-\frac{1}{2}\left(\frac{d_0ut}{h(t)}\right)^2-d_1t+\mathtt{i}d_2th(t)+\mathcal{O}\left(th^2(t)+\frac{t^2}{h(t)}\right),$$

where $g_3 := g_1^2 + \mathtt{i}g_2(1-g_0)$. Consequently,

$$\begin{aligned}
&\frac{1-\left(g_0-\mathtt{i}g_1h(t)/u-\mathtt{i}g_2h^2(t)/u^2+\mathcal{O}(h^3(t))\right)\mathrm{e}^{-\mathtt{i}d_0ut/h(t)-d_1t+\mathcal{O}(th(t))}}{1-g_0+\mathtt{i}g_1h(t)/u+\mathtt{i}g_2h^2(t)/u^2+\mathcal{O}(h^3(t))}\\
&=\left\{1-\left[g_0-\frac{\mathtt{i}g_1}{u}h(t)-\frac{\mathtt{i}g_2}{u^2}h^2(t)+\mathcal{O}(h^3(t))\right]\right\}\\
&\quad\left[1-\frac{\mathtt{i}d_0ut}{h(t)}-\frac{1}{2}\left(\frac{d_0ut}{h(t)}\right)^2-d_1t+\mathtt{i}d_2th(t)+\mathcal{O}\left(th^2(t)+\frac{t^2}{h(t)}\right)\right]\\
&\quad\frac{1}{1-g_0}\left(1-\frac{\mathtt{i}g_1h(t)}{u(1-g_0)}-\frac{g_3h^2(t)}{u^2(1-g_0)^2}+\mathcal{O}(h^3(t))\right)\\
&=\left(1+\frac{\mathtt{i}g_0d_0ut}{(1-g_0)h(t)}+\frac{\mathtt{i}g_1h(t)}{u(1-g_0)}+\frac{d_1g_0+d_0g_1}{1-g_0}t+\frac{\mathtt{i}g_2h^2(t)}{u^2(1-g_0)}+\frac{g_0d_0^2u^2t^2}{2(1-g_0)h^2(t)}+\mathcal{O}\left(th(t)+h^3(t)+\frac{t^2}{h(t)}\right)\right)\\
&\quad\left(1-\frac{\mathtt{i}g_1h(t)}{u(1-g_0)}-\frac{g_3h^2(t)}{u^2(1-g_0)^2}+\mathcal{O}\left(h^3(t)\right)\right)\\
&=1+\frac{\mathtt{i}g_0d_0u}{1-g_0}\frac{t}{h(t)}+\frac{u^2d_0^2g_0t^2}{2(1-g_0)h^2(t)}+\left(\frac{d_1g_0+d_0g_1}{1-g_0}+\frac{d_0g_0g_1}{(1-g_0)^2}\right)t+\mathcal{O}\left(th(t)+h^3(t)+\frac{t^2}{h(t)}\right),
\end{aligned}$$

and therefore

$$\begin{aligned}
&\log\left(\frac{1-\left[g_0-\mathtt{i}h(t)g_1/u-\mathtt{i}h^2(t)g_2/u^2+\mathcal{O}(h^3(t))\right]\mathrm{e}^{-\mathtt{i}d_0ut/h(t)-d_1t+\mathcal{O}(th(t))}}{1-g_0+\mathtt{i}h(t)g_1/u+\mathtt{i}h^2(t)g_2/u^2+\mathcal{O}(h^3(t))}\right)\\
&=\frac{\mathtt{i}g_0d_0u}{1-g_0}\frac{t}{h(t)}+\frac{u^2d_0^2g_0}{2(1-g_0)^2}\frac{t^2}{h^2(t)}+\left(\frac{d_1g_0+d_0g_1}{1-g_0}+\frac{d_0g_0g_1}{(1-g_0)^2}\right)t+\mathcal{O}\left(th(t)+h^3(t)+\frac{t^2}{h(t)}+\frac{t^3}{h^3(t)}\right).
\end{aligned}$$

Plugging this into (C.6), the result follows by noticing that the coefficients of $\frac{t}{h(t)}$ and t are both zero. ∎

Appendix D. Proofs of the main results.

D.1. Proof of Proposition 4.1. In [39, section 6] the authors proved that $\mathcal{D}^* = \mathbb{R}$ whenever $\gamma < 1$, and $\mathcal{D}^* = (u_-, u_+)$ if $\gamma = 1$. Throughout the proof we keep the notation h, emphasizing that the statement still holds for function h with a general form, not only polynomials.

Case $\gamma \in (0, 1/2)$. We need to analyze the behavior of $\log \mathrm{M}(z)$ as z approaches zero. Since $\mathfrak{m}$ is strictly positive, by continuity of the mgf around the origin, $\mathrm{M}_{\mathcal{V}}\big(u^2t(2h^2(t))^{-1}(1+$

$\mathcal{O}(h(t))\big)$ converges to $\mathrm{M}_{\mathcal{V}}(0) = 1$ as t tends to zero for any u in $\mathbb{R}$, which implies that $\mathcal{D}^*_{\mathcal{V}} = \mathbb{R}$. For small t, a Taylor expansion indicates that

$$\begin{aligned}\log \mathrm{M}_{\mathcal{V}}\left(\mathrm{D}\left(t, \frac{u}{h(t)}\right)\right) &= \log \mathbb{E}\left(\exp\left\{\frac{u^2 t\mathcal{V}}{2h^2(t)}\left[1 - \frac{h(t)}{u} + \mathcal{O}\left(\frac{t}{h(t)}\right) + \mathcal{O}\left(h^2(t)\right)\right]\right\}\right) \\ &= \log\left\{1 + \frac{u^2\mathbb{E}(\mathcal{V})t}{2h^2(t)}\left[1 - \frac{h(t)}{u} + \mathcal{O}\left(\frac{t}{h(t)} + h^2(t)\right)\right] + \frac{u^4\mathbb{E}(\mathcal{V}^2)t^2}{8h^4(t)} + \mathcal{O}\left(\frac{t^3}{h^6(t)}\right)\right\} \\ &= \frac{u^2\mathbb{E}(\mathcal{V})t}{2h^2(t)}\left(1 + \mathcal{O}\left(h(t) + \frac{t}{h^2(t)}\right)\right).\end{aligned}$$

Since $h(t)\mathrm{C}(t, u/h(t))$ is of order $\mathcal{O}\left(t^2/h(t) + h^4(t)\right)$, then

$$\Lambda_\gamma\left(t, \frac{u}{h(t)}\right) = \frac{u^2\mathbb{E}(\mathcal{V})t}{2h(t)}\left\{1 + \mathcal{O}\left(h(t) + \frac{t}{h^2(t)} + h^4(t)\right)\right\}, \tag{D.1}$$

and therefore $\lim_{t\downarrow 0}\Lambda_\gamma(t, u/h(t)) = 0$ for all $u \in \mathbb{R}$.

Case $\gamma \in (1/2, 1]$. We need to evaluate $\mathrm{M}_{\mathcal{V}}$ at infinity. If $\mathfrak{m}$ is finite, for t sufficiently small, the term $\mathrm{M}_{\mathcal{V}}\left(\frac{1}{2}u^2 t h^{-2}(t)\left(1 + \mathcal{O}\left(t/h(t)\right)\right)\right)$ is infinite for any nonzero u; hence $\mathcal{D}^*_{\mathcal{V}} = \{0\}$, and $\Lambda_\gamma(u)$ is null at $u = 0$, and is infinite elsewhere. If $\mathfrak{m}$ is infinite, then obviously $\mathcal{D}^*_{\mathcal{V}} = \mathbb{R}$. Assume first that $\mathfrak{v}_+$ is finite; we claim that $\lim_{u\uparrow\infty}(\mathfrak{v}_+ u)^{-1}\log \mathrm{M}_{\mathcal{V}}(u) = 1$. In fact, let $F_{\mathcal{V}}$ be the cumulative distribution function of $\mathcal{V}$. Then

$$\mathrm{M}_{\mathcal{V}}(u) = \mathbb{E}\left(\mathrm{e}^{u\mathcal{V}}\right) \leq \exp(u\mathfrak{v}_+)\int_{[\mathfrak{v}_-, \mathfrak{v}_+]} F_{\mathcal{V}}(\mathrm{d}v) = \exp(u\mathfrak{v}_+).$$

For any small $\varepsilon > 0$, fix $\delta \in (0, \varepsilon\mathfrak{v}_+/2)$, so that

$$\begin{aligned}\frac{\log \mathrm{M}_{\mathcal{V}}(u)}{u\mathfrak{v}_+} &\geq \frac{1}{u\mathfrak{v}_+}\log\left(\int_{\mathfrak{v}_+ - \delta}^{\mathfrak{v}_+} \mathrm{e}^{uv} F_{\mathcal{V}}(\mathrm{d}v)\right) \\ &\geq \frac{1}{u\mathfrak{v}_+}\log\left(\mathrm{e}^{u(\mathfrak{v}_+ - \delta)}\mathbb{P}\left(\mathcal{V} \geq \mathfrak{v}_+ - \delta\right)\right) = 1 - \frac{\delta}{\mathfrak{v}_+} + \frac{\log \mathbb{P}\left(\mathcal{V} \geq \mathfrak{v}_+ - \delta\right)}{u\mathfrak{v}_+},\end{aligned}$$

since $\mathfrak{v}_+$ is the upper bound of the support; therefore $\mathbb{P}(\mathcal{V} \geq \mathfrak{v}_+ - \delta)$ is strictly positive, and the result follows. If $\gamma \in (1/2, 1)$, notice that $h(t)\mathrm{C}(t, u/h(t))$ is of order $t^{2-\gamma}$ from Lemma C.4, and hence

$$\begin{aligned}\lim_{t\downarrow 0}\Lambda_\gamma\left(t, \frac{u}{h(t)}\right) &= \lim_{t\downarrow 0}\mathcal{O}\left(t^{2-\gamma}\right) + \lim_{t\downarrow 0} t^\gamma \log \mathrm{M}_{\mathcal{V}}\left(\frac{u^2 t^{1-2\gamma}}{2}\left(1 + \mathcal{O}(t^{1-\gamma})\right)\right) \\ &= \frac{u^2\mathfrak{v}_+}{2}\lim_{t\downarrow 0} t^{1-\gamma} = 0 \quad \text{for any } u \text{ in } \mathbb{R}.\end{aligned}$$

When $\gamma = 1$, $\Lambda(u)$ is positive whenever $u \in (u_-, u_+) \setminus \{0\}$. Therefore,

$$\lim_{t\downarrow 0}\Lambda_\gamma\left(t, \frac{u}{h(t)}\right) = \lim_{t\downarrow 0}\mathcal{O}(t) + \lim_{t\downarrow 0} t\left(\frac{\mathfrak{v}_+\Lambda(u)}{t}(1 + \mathcal{O}(t))\right) = \Lambda(u)\mathfrak{v}_+ \quad \text{for any } u \in \mathcal{D}^* = (u_-, u_+).$$

Case $\gamma = 1/2$. If $\mathfrak{v}_+$ is finite, then the pointwise limit is null on the whole real line. Assume now that $\mathfrak{v}_+$ is infinite and $\mathfrak{m}$ is finite. Following Remark C.3(iii), $\frac{u^2}{2} + \left(\frac{\rho\xi u^3}{4} - \frac{u}{2}\right)t^{1/2} + \mathcal{O}(t) < \mathfrak{m}$ implies $\mathcal{D}_{\mathcal{V}}^{*o} = \left(-\sqrt{2\mathfrak{m}}, \sqrt{2\mathfrak{m}}\right) \subseteq \mathcal{D}_{\mathcal{V}}^{*} \subseteq \limsup_{t\downarrow 0} \mathcal{D}_{\mathcal{V}}^{t} \subseteq \left[-\sqrt{2\mathfrak{m}}, \sqrt{2\mathfrak{m}}\right] = \overline{\mathcal{D}_{\mathcal{V}}^{*}}$. For sufficiently small t,

$$\Lambda_{1/2}\left(t, \frac{u}{\sqrt{t}}\right) = \frac{\kappa\theta u^2}{4} t^{3/2} + \mathcal{O}\left(t^2\right) + t^{1/2} \log \mathrm{M}_{\mathcal{V}}\left(\frac{u^2}{2} + \left(\frac{\rho\xi u^3}{4} - \frac{u}{2}\right) t^{1/2} + \mathcal{O}(t)\right).$$

For any fixed u in $\mathcal{D}_{\mathcal{V}}^{*o}$, by definition there exists a positive t_0 such that u is in $\mathcal{D}_{\mathcal{V}}^{t}$ for all t less than t_0. Then the mgf of $\mathcal{V}$ is infinitely differentiable around the point $u^2/2$, and the nth order derivative at this point is $\mathrm{M}_{\mathcal{V}}^{(n)}\left(\frac{1}{2}u^2\right) = \mathbb{E}\left[\mathcal{V}^n \exp\left(\frac{1}{2}u^2\mathcal{V}\right)\right]$. Denote now $a_n(u) := \mathrm{M}_{\mathcal{V}}^{(n)}\left(\frac{1}{2}u^2\right) \mathrm{M}_{\mathcal{V}}^{-1}\left(\frac{1}{2}u^2\right)$ for $n \in \mathbb{N}_+$, and $a_0(u) := \log \mathrm{M}_{\mathcal{V}}\left(\frac{1}{2}u^2\right)$. A Taylor expansion of the function $\mathrm{M}_{\mathcal{V}}$ around the point $\frac{1}{2}u^2$ yields

$$\begin{aligned}\Lambda_{1/2}\left(t, \frac{u}{\sqrt{t}}\right) &= \sqrt{t} \log\left\{\mathrm{M}_{\mathcal{V}}\left(\frac{u^2}{2}\right)\left[1 + a_1(u)\left(\frac{\rho\xi u^2}{2} - 1\right)\frac{u\sqrt{t}}{2} + \mathcal{O}(t)\right]\right\} + \frac{\kappa\theta u^2}{4} t^{3/2} + \mathcal{O}\left(t^2\right) \\ &= a_0(u)\sqrt{t} + a_1(u)\left(\frac{\rho\xi u^2}{2} - 1\right)\frac{ut}{2} + \mathcal{O}(t^{3/2}). \qquad \text{(D.2)}\end{aligned}$$

Letting t tend to zero, we finally obtain

$$\Lambda_{1/2}(u) = \begin{cases} 0 & \text{when } u \in \mathcal{D}_{\mathcal{V}}^{*o}, \\ \infty & \text{when } u \in \mathbb{R} \setminus \overline{\mathcal{D}_{\mathcal{V}}^{*}}. \end{cases}$$

However, the limit of $\Lambda_{1/2}\left(t, \pm\sqrt{2\mathfrak{m}/t}\right)$ depends on the explicit form of $\mathrm{M}_{\mathcal{V}}$. To see this, assume that $\rho\xi\mathfrak{m} < 1$, which is guaranteed in particular when $\rho \leq 0$, and compute the limit when $u = \sqrt{2\mathfrak{m}}$. L'Hôpital's rule implies

$$\lim_{t\downarrow 0} t^{1/2} \log \mathrm{M}_{\mathcal{V}}\left(\mathfrak{m} + \sqrt{\frac{\mathfrak{m}}{2}}\left(\rho\xi\mathfrak{m} - 1\right) t^{1/2} + \mathcal{O}(t)\right) = \sqrt{\frac{2}{\mathfrak{m}}} \frac{1}{1 - \rho\xi\mathfrak{m}} \lim_{s\downarrow 0} \frac{s^2 \mathrm{M}_{\mathcal{V}}'(\mathfrak{m} - s)}{\mathrm{M}_{\mathcal{V}}(\mathfrak{m} - s)}. \qquad \text{(D.3)}$$

D.2. Proof of Theorem 4.11. The systematic procedure is similar to the proof of [39, Theorem 3.1]. To simplify notation, write $\widetilde{\Lambda}_t(u) := \Lambda_{1/2}\left(t, u/\sqrt{t}\right)$, $\widetilde{\mathrm{C}}_t(u) := \mathrm{C}(t, u/\sqrt{t})$, and $\widetilde{\mathrm{D}}_t(u) := \mathrm{D}(t, u/\sqrt{t})$ whenever these quantities are well defined. We shall prove the theorem in several steps: In Lemma D.1 we show that a saddle point analysis is feasible; by taking the expectation under a new probability measure, the main contribution of the option price arises, and its asymptotic expansion is provided in Lemma D.2; in Lemma D.3 we prove the convergence (with rescaling) of the sequence $(X_t - x)_{t\geq 0}$ under this new measure; finally, the full asymptotics of the call option price is obtained via inverse Fourier transform.

Lemma D.1. *Under Assumption 4.8, for any $x \neq 0$, $t > 0$ small enough, the equation $\partial_u \widetilde{\Lambda}_t(u) = x$ admits a unique solution $u_t^*(x)$ such that $\widetilde{\mathrm{D}}_t(u_t^*(x)) \in \mathcal{D}_{\mathcal{V}}^{t}$, and the following holds as t tends to zero:*

$$u_t^*(x) = \begin{cases} \operatorname{sgn}(x)\sqrt{2\mathfrak{m}} + b_1(x) t^{\frac{1}{2\omega}} + o\left(t^{\frac{1}{2\omega}}\right) & \text{for } \omega = 1, \\ \operatorname{sgn}(x)\sqrt{2\mathfrak{m}} + b_1(x) t^{\frac{1}{2\omega}} + b_2(x) t^{\frac{1}{\omega}} \log t + b_3(x) t^{\frac{1}{\omega}} + o\left(t^{\frac{1}{\omega}}\right) & \text{for } \omega \geq 2, \end{cases}$$

where

$$b_1(x) := -\mathrm{sgn}(x)(2\mathfrak{m})^{(1-\omega)/(2\omega)}\left(\frac{\mathbf{1}_{\{\omega=1\}}|\gamma_0| + \mathbf{1}_{\{\omega\geq 2\}}(\omega-1)\gamma_0}{|x|}\right)^{1/\omega} + \frac{1-\rho\xi\mathfrak{m}}{2}\mathbf{1}_{\{\omega=1\}},$$

$$b_2(x) := -\mathrm{sgn}(x)\frac{\mathfrak{a}\sqrt{2\mathfrak{m}}}{2\omega^2}b_1^2(x),$$

$$b_3(x) := \mathrm{sgn}(x)\left\{\frac{b_1^2(x)}{\sqrt{2\mathfrak{m}}\omega}\left(1-\frac{\omega}{2}-2\mathfrak{a}\mathfrak{m}\log\left(\sqrt{2\mathfrak{m}}|b_1(x)|\right)-2\mathfrak{b}\mathfrak{m}\right)\right\} + \frac{1-\rho\xi\mathfrak{m}}{2}\mathbf{1}_{\{\omega=2\}}.$$

If $x=0$, then $u_t^*(0)$ defined as the solution to $\partial_u\widetilde{\Lambda}_t(u)=0$ satisfies $u_t^*(0)=\frac{1}{2}\sqrt{t}+o(\sqrt{t})$.

Proof of Lemma D.1. Assume that $x>0$, the case when $x<0$ being analogous. Equation (2.3) implies that for any $u\in\mathbb{R}$, the equation $\partial_u\widetilde{\Lambda}_t(u)=x$ reads

$$x=\partial_u\widetilde{\Lambda}_t(u)=\sqrt{t}\left(\log \mathrm{M}\left(t,\frac{u}{\sqrt{t}}\right)\right)'=\sqrt{t}\widetilde{\mathrm{C}}_t'(u)+\sqrt{t}\frac{\mathrm{M}_{\mathcal{V}}'\left(\widetilde{\mathrm{D}}_t(u)\right)}{\mathrm{M}_{\mathcal{V}}\left(\widetilde{\mathrm{D}}_t(u)\right)}\widetilde{\mathrm{D}}_t'(u). \tag{D.4}$$

The existence and uniqueness of the solution to (D.4) are guaranteed by the strict convexity of the rescaled cgf $\widetilde{\Lambda}_t$ for each t [43, Theorem 2.3] and (4.8), in which the denominator tends to zero as u tends to the boundary of $\mathcal{D}_{\mathcal{V}}^t$. Denote now the unique solution by $u_t^*(x)$. Applying Lemmas C.2 and C.4 with $h(t)\equiv t^{1/2}$,

$$\widetilde{\mathrm{C}}_t'(u)=\frac{u\kappa\theta}{2}t+\mathcal{O}\left(t^{\frac{3}{2}}\right)\quad\text{and}\quad\widetilde{\mathrm{D}}_t'(u)=u+\left(\frac{3\rho\xi u^2}{4}-\frac{1}{2}\right)\sqrt{t}+\mathcal{O}(t).$$

We first prove that $\lim_{t\downarrow 0}u_t^*(x)=\sqrt{2\mathfrak{m}}$. If $\lim_{t\downarrow 0}u_t^*(x)\neq\sqrt{2\mathfrak{m}}$, there exist a sequence $\{t_n\}_{n=1}^{\infty}$ and (small enough) $\varepsilon_0>0$ satisfying $\lim_{n\uparrow\infty}t_n=0$ and $|u_{t_n}^*(x)-\sqrt{2\mathfrak{m}}|\geq\varepsilon_0$ for any $n\geq 1$. In section D.1 it is proved that $\lim_{t\downarrow 0}\mathcal{D}_{\mathcal{V}}^t\subseteq\limsup_{t\downarrow 0}\mathcal{D}_{\mathcal{V}}^t\subseteq\overline{\mathcal{D}_{\mathcal{V}}^*}=[-\sqrt{2\mathfrak{m}},\sqrt{2\mathfrak{m}}]$. Also notice that for any fixed t small enough, the map $\partial_u\widetilde{\Lambda}_t:\mathcal{D}_{\mathcal{V}}^t\to\mathbb{R}$ is continuous and strictly increasing. Hence for fixed positive ε_0 there are at most finitely many t_i in the sequence such that $u_{t_i}^*(x)\geq\sqrt{2\mathfrak{m}}+\varepsilon_0$.

Equation (D.4) implies that for fixed $x>0$ the limit of $t^{-1/2}\partial_u\widetilde{\Lambda}_t(u_t^*(x))$ is infinity as t tends to zero. Taking a subsequence of $\{t_n\}_{n\geq 1}$ if necessary, assume now that $u_{t_n}^*(x)\leq\sqrt{2\mathfrak{m}}-\varepsilon_0$ for any $n\geq 1$. Since $\widetilde{\mathrm{D}}_t(\sqrt{2\mathfrak{m}}-\varepsilon)=\mathfrak{m}-\sqrt{2\mathfrak{m}}\varepsilon+\varepsilon^2/2+\mathcal{O}(\sqrt{t})$, then for any $\varepsilon>0$ there exists $N(\varepsilon)\in\mathbb{N}$ such that $\left|\widetilde{\mathrm{D}}_{t_n}(\sqrt{2\mathfrak{m}}-\varepsilon)-\mathfrak{m}+\sqrt{2\mathfrak{m}}\varepsilon-\varepsilon^2/2\right|<\sqrt{2\mathfrak{m}}\varepsilon/2$ holds for any $n\geq N(\varepsilon)$. Fix $0<\varepsilon_1<\min(\varepsilon_0,\sqrt{2\mathfrak{m}})$ small enough so that $\mathfrak{m}-3\sqrt{2\mathfrak{m}}\varepsilon_1/2+\varepsilon_1^2/2>\mathfrak{m}-\delta_0$, where $\delta_0>0$ is chosen such that, for any $\mathfrak{m}-\delta_0<u<\mathfrak{m}$, the higher-order term in (4.8) is bounded above by one. Then for such ε_1 and for any $n\geq N(\varepsilon_1)$ we have $\mathfrak{m}-\delta_0<\widetilde{\mathrm{D}}_{t_n}(\sqrt{2\mathfrak{m}}-\varepsilon_1)<\mathfrak{m}-\sqrt{2\mathfrak{m}}\varepsilon_1/2+\varepsilon_1^2/2<\mathfrak{m}$. The function $\partial_u\widetilde{\Lambda}_t$ is strictly increasing, implying

$$\lim_{n\uparrow\infty}\frac{\partial_u\widetilde{\Lambda}_{t_n}\left(u_{t_n}^*(x)\right)}{\sqrt{t_n}}\leq\lim_{n\uparrow\infty}\frac{\partial_u\widetilde{\Lambda}_{t_n}\left(\sqrt{2\mathfrak{m}}-\varepsilon_1\right)}{\sqrt{t_n}}\leq\frac{2^{\omega+1}\delta_1}{\varepsilon_1^{\omega}(\sqrt{2\mathfrak{m}}-\varepsilon_1)^{\omega-1}}<\infty,$$

where $\delta_1:=\mathbf{1}_{\{\omega=1\}}|\gamma_0|+\mathbf{1}_{\{\omega\geq 2\}}(\omega-1)\gamma_0$, hence the contradiction. Therefore $\lim_{t\downarrow 0}u_t^*(x)=\sqrt{2\mathfrak{m}}$. Analogously we can prove that $\lim_{t\downarrow 0}u_t^*(0)=0$.

Case $\omega = 1$. Assume that $u_t^*(x) = \sqrt{2\mathfrak{m}} + h_x(t)$, where $h_x(t) = o(1)$. Equation (D.4) implies that $h_x(t) = \mathcal{O}\left(\sqrt{t}\right)$, and hence all the terms of order $\mathcal{O}(\sqrt{t})$ in the expansion of $\widetilde{\mathrm{D}}_t(u_t^*(x))$ should be included. More specifically,

$$\widetilde{\mathrm{D}}_t\left(u_t^*(x)\right) = \mathfrak{m} + \sqrt{2\mathfrak{m}}h_x(t) + \frac{\sqrt{2\mathfrak{m}}}{2}\left(\rho\xi\mathfrak{m} - 1\right)\sqrt{t} + o(\sqrt{t}).$$

Plugging this back into (D.4) and solving at the leading order yields the desired result.

Case $\omega \geq 2$. In this case $h_x(t) = \mathcal{O}(t^{1/(2\omega)})$. Equation (D.4) now reads

(D.5)
$$\frac{\sqrt{t}}{x}\left\{\frac{\kappa\theta\sqrt{2\mathfrak{m}}}{2}t + \frac{\kappa\theta}{2}th_x(t) + \mathcal{O}\left(t^{3/2}\right) + \left(\frac{\delta_0(1+o(1))}{\left(-\sqrt{2\mathfrak{m}}h_x(t) + \mathcal{O}\left(h_x^2 + \sqrt{t}\right)\right)^{\omega}}\right)\left(\sqrt{2\mathfrak{m}} + h_x(t) + \mathcal{O}\left(\sqrt{t}\right)\right)\right\} \equiv 1.$$

Denote by h_x^* the leading order of the function h_x. Solving (D.5) at the leading order, we obtain $\delta_0\sqrt{2\mathfrak{m}t} \equiv x\left(-\sqrt{2\mathfrak{m}}h_x^*(t)\right)^{\omega}$, from which $h_x^*(t) = -\left(2\mathfrak{m}\right)^{\frac{1-\omega}{2\omega}}\left(\delta_0/x\right)^{\frac{1}{\omega}}t^{\frac{1}{2\omega}}$. Higher orders in the expansion of $u_t^*(x)$ can be derived similarly, simply by replacing the little-o term in (D.5) with precise higher-order terms provided in (4.8). We omit the details.

Finally, when $x = 0$, write $u_t^*(0) = h(t)$ with $h(t) = o(1)$. As t tends to zero, $\mathrm{M}_{\mathcal{V}}(u_t^*(0)) \sim 1$, $\mathrm{M}'_{\mathcal{V}}(u_t^*(0)) \sim \mathbb{E}(\mathcal{V})$, and $\widetilde{\mathrm{D}}'_t\left(u_t^*(0)\right) = h(t) - \frac{1}{2}\sqrt{t} + \mathcal{O}\left(t + h^2(t)\sqrt{t}\right)$. Plugging these into (D.4) with $x = 0$ proves the lemma. ∎

Lemma D.2.

1. *When $\gamma_0 > 0$ and $\omega \geq 2$, as t tends to zero,*

$$\exp\left(\frac{-xu_t^*(x) + \widetilde{\Lambda}_t(u_t^*(x))}{\sqrt{t}}\right) = \exp\left(-\frac{\Lambda^*(x)}{\sqrt{t}} + c_1(x)t^{\frac{1-\omega}{2\omega}} + o\left(t^{\frac{1-\omega}{2\omega}}\right)\right)$$

   for any $x \neq 0$, where $c_1(x) := \omega\gamma_0^{1/\omega}\left(\frac{|x|}{\sqrt{2\mathfrak{m}}(\omega-1)}\right)^{1-1/\omega}$, and the function Λ^* is defined in (4.9).

2. *If $\gamma_0 < 0$ and $\omega = 1$, then for any $x \neq 0$, as t tends to zero,*

$$\exp\left(\frac{-xu_t^*(x) + \widetilde{\Lambda}_t(u_t^*(x))}{\sqrt{t}}\right) = \exp\left(-\frac{\Lambda^*(x)}{\sqrt{t}} + c_2(x) + \gamma_1\right)\left(\frac{|x|}{|\gamma_0|\sqrt{2\mathfrak{m}t}}\right)^{|\gamma_0|}(1 + o(1)),$$

   where $c_2(x) := \frac{1}{2}\left(\rho\xi\mathfrak{m} - 1\right)x - \gamma_0$.

Proof of Lemma D.2.

Case $\omega \geq 2$. Assumption 4.8 and Lemma D.1 imply

$$\begin{aligned}
\exp\left(-\frac{xu_t^*(x)}{\sqrt{t}}\right) &= \exp\left\{-\frac{x}{\sqrt{t}}\left[\sqrt{2\mathfrak{m}} + b_1(x)t^{\frac{1}{2\omega}} + o(t^{\frac{1}{2\omega}})\right]\right\} \\
&= \exp\left\{-\frac{\Lambda^*(x)}{\sqrt{t}} - b_1(x)xt^{\frac{1-\omega}{2\omega}} + o\left(t^{\frac{1-\omega}{2\omega}}\right)\right\}, \\
\exp\left(\frac{\widetilde{\Lambda}_t(u_t^*(x))}{\sqrt{t}}\right) &= \exp\left(\widetilde{\mathrm{C}}_t(u_t^*) + \log\mathrm{M}_{\mathcal{V}}(\widetilde{\mathrm{D}}_t(u_t^*))\right) = \exp\left\{\frac{\gamma_0}{\left(\sqrt{2\mathfrak{m}}|b_1(x)|\right)^{\omega-1}}t^{\frac{1-\omega}{2\omega}} + o\left(t^{\frac{1-\omega}{2\omega}}\right)\right\}.
\end{aligned}$$

Using the expression of $b_1(\cdot)$ provided in Lemma D.1, the coefficient of the term of order $t^{\frac{1-\omega}{2\omega}}$ is given by

$$-b_1(x)x + \frac{\gamma_0}{\left(\sqrt{2\mathfrak{m}}|b_1|\right)^{\omega-1}} = \left\{[(\omega-1)\gamma_0]^{\frac{1}{\omega}} + \gamma_0[(\omega-1)\gamma_0]^{\frac{1-\omega}{\omega}}\right\}\left(\sqrt{2\mathfrak{m}}\right)^{\frac{1-\omega}{\omega}}|x|^{1-\frac{1}{\omega}}$$
$$= \omega\gamma_0^{\frac{1}{\omega}}\left(\frac{|x|}{\sqrt{2\mathfrak{m}}(\omega-1)}\right)^{1-\frac{1}{\omega}} = c_1(x).$$

Case $\omega = 1$. This case follows by straightforward computations after noticing that

$$\exp\left\{\frac{\widetilde{\Lambda}_t(u_t^*(x))}{\sqrt{t}}\right\} = \exp\left\{\mathcal{O}(t) + \gamma_0\log\left(\mathfrak{m} - \widetilde{\mathrm{D}}_t(u_t^*(x))\right) + \gamma_1 + o(1)\right\}$$
$$= \mathrm{e}^{\gamma_1}\left(\frac{|\gamma_0|\sqrt{2\mathfrak{m}t}}{|x|}\right)^{\gamma_0}(1+o(1))\,. \qquad \blacksquare$$

For each $x \neq 0$ and $t > 0$ small enough, define the time-dependent measure $\mathbb{Q}_t$ by

$$\frac{\mathrm{d}\mathbb{Q}_t}{\mathrm{d}\mathbb{P}} := \exp\left(\frac{u_t^*(x)X_t - \widetilde{\Lambda}_t(u_t^*(x))}{t^{1/2}}\right).$$

Lemma D.1 implies that $\widetilde{\Lambda}_t(u_t^*(x))$ is finite for small t. Also, by definition it is obvious that $\mathbb{E}[\mathrm{d}\mathbb{Q}_t/\mathrm{d}\mathbb{P}] = 1$; then $\mathbb{Q}_t$ is a well-defined probability measure for each t.

Lemma D.3. *For any $x \neq 0$, let $Z_t := (X_t - x)/\vartheta(t)$, where $\vartheta(t) := \mathbf{1}_{\{\omega=1\}} + \mathbf{1}_{\{\omega=2\}}t^{1/8}$. Under Assumption 4.8, as t tends to zero, the characteristic function of Z_t under $\mathbb{Q}_t$ is*

$$\Psi_t(u) := \mathbb{E}^{\mathbb{Q}_t}\left(\mathrm{e}^{\mathrm{i}uZ_t}\right) = \begin{cases} \mathrm{e}^{-\mathrm{i}ux}\left(1 - \dfrac{\mathrm{i}ux}{|\gamma_0|}\right)^{\gamma_0}(1+o(1)) & \text{for } \omega = 1, \\ \exp\left(\dfrac{-u^2\zeta^2(x)}{2}\right)(1+o(1)) & \text{for } \omega = 2, \end{cases}$$

where $\zeta(x) := \sqrt{2}\left(\frac{2\mathfrak{m}}{\gamma_0^2}\right)^{1/8}|x|^{3/4}$.

Remark D.4. *Lemma D.3 and Lévy's convergence theorem* [50, Theorem 18.1] *imply that under $\mathbb{Q}_t$ the process $(Z_t)_{t\geq 0}$ converges weakly to a Gamma distribution (or a Gamma distribution mirrored to the negative real half line) if $x > 0$ (or $x < 0$) minus the constant x when $\omega = 1$, and to a Gaussian distribution when $\omega = 2$.*

Remark D.5. *Intuitively, the case $\omega \geq 3$ should be similar to the case $\omega = 2$, so that a suitable candidate for the function ϑ can be found. However, in such a scenario more information on the asymptotics of $\log \mathrm{M}_{\mathcal{Y}}$ and its derivative are required in order to obtain the suitable (nonconstant) characteristic function. These extra assumptions turn out to be very restrictive and of little practical use, and are thus omitted.*

Proof of Lemma D.3. Assume that $x > 0$, with $x < 0$ being analogous. Function $\log \Psi_t$ can be written as

$$\begin{aligned}(\text{D.6}) \qquad \log \Psi_t(u) &= \log \mathbb{E}\left[\exp\left(\frac{\mathtt{i}u(X_t - x)}{\vartheta(t)} + \frac{u_t^*(x)X_t - \widetilde{\Lambda}_t(u_t^*(x))}{\sqrt{t}}\right)\right] \\ &= -\frac{\mathtt{i}ux}{\vartheta(t)} + \log \mathbb{E}\left[\exp\left(\frac{\left(\mathtt{i}u\sqrt{t}/\vartheta(t) + u_t^*(x)\right)X_t}{\sqrt{t}}\right)\right] - \frac{\widetilde{\Lambda}_t(u_t^*(x))}{\sqrt{t}} \\ &= -\frac{\mathtt{i}ux}{\vartheta(t)} + \frac{1}{\sqrt{t}}\left(\widetilde{\Lambda}_t\left(u_t^*(x) + \mathtt{i}u\sqrt{t}/\vartheta(t)\right) - \widetilde{\Lambda}_t\left(u_t^*(x)\right)\right).\end{aligned}$$

Case $\omega = 1$. Lemma D.1 implies that

$$\begin{aligned}\widetilde{\mathrm{D}}_1(u) &:= \widetilde{\mathrm{D}}_t\left(u_t^*(x) + \frac{\mathtt{i}u\sqrt{t}}{\vartheta(t)}\right) = \mathfrak{m} + \frac{\gamma_0\sqrt{2\mathfrak{m}t}}{x} + \mathtt{i}u\sqrt{2\mathfrak{m}t} + o(\sqrt{t}), \\ \widetilde{\mathrm{D}}_2 &:= \widetilde{\mathrm{D}}(u_t^*(x)) = \mathfrak{m} + \frac{\gamma_0\sqrt{2\mathfrak{m}t}}{x} + o(\sqrt{t}), \\ \widetilde{\mathrm{C}}_1(u) &:= \widetilde{\mathrm{C}}\left(u_t^*(x) + \frac{\mathtt{i}u\sqrt{t}}{\vartheta(t)}\right) = \frac{\mathfrak{m}\kappa\theta t}{2} + \mathcal{O}\left(t^{3/2}\right), \\ \widetilde{\mathrm{C}}_2 &:= \widetilde{\mathrm{C}}(u_t^*(x)) = \frac{\mathfrak{m}\kappa\theta t}{2} + \mathcal{O}\left(t^{3/2}\right).\end{aligned}$$

As a result, the lemma follows in this case from the following computations:

$$\begin{aligned}\log \Psi_t(u) &= -\mathtt{i}ux + \widetilde{\mathrm{C}}_1(u) - \widetilde{\mathrm{C}}_2 + \log \mathrm{M}_{\mathcal{V}}\left(\widetilde{\mathrm{D}}_1(u)\right) - \log \mathrm{M}_{\mathcal{V}}\left(\widetilde{\mathrm{D}}_2\right) \\ &= -\mathtt{i}ux + \gamma_0 \log\left(\frac{\mathfrak{m} - \widetilde{\mathrm{D}}_1(u)}{\mathfrak{m} - \widetilde{\mathrm{D}}_2}\right) + o(1) \\ &= -\mathtt{i}ux + \gamma_0 \log\left(1 - \frac{\mathtt{i}ux}{|\gamma_0|} + o(1)\right) + o(1).\end{aligned}$$

Case $\omega = 2$. Denote $\theta := 1/8$. Then $\frac{1}{2} - \theta > \frac{1}{4} = \frac{1}{2\omega}$. Lemma D.1 implies

$$\begin{aligned}\widetilde{\mathrm{D}}_1(u) &= \mathfrak{m} + \sqrt{2\mathfrak{m}}b_1 t^{1/4} + \mathtt{i}u\sqrt{2\mathfrak{m}}t^{1/2-\theta} + \left(\frac{b_1^2}{2} + \sqrt{2\mathfrak{m}}b_3 + \sqrt{\frac{\mathfrak{m}}{2}}(\mathfrak{m}\rho\xi - 1)\right)t^{1/2} + o(\sqrt{t}), \\ \widetilde{\mathrm{D}}_2 &= \mathfrak{m} + \sqrt{2\mathfrak{m}}b_1 t^{1/4} + \left(\frac{b_1^2}{2} + \sqrt{2\mathfrak{m}}b_3 + \sqrt{\frac{\mathfrak{m}}{2}}(\mathfrak{m}\rho\xi - 1)\right)t^{1/2} + o(\sqrt{t}), \\ \widetilde{\mathrm{C}}_1(u) &= \frac{\mathfrak{m}\kappa\theta t}{2} + \frac{\kappa\theta\sqrt{2\mathfrak{m}}b_1}{2}t^{5/4} + \mathcal{O}\left(t^{11/8}\right), \quad \text{and} \quad \widetilde{\mathrm{C}}_2 = \frac{\mathfrak{m}\kappa\theta t}{2} + \frac{\kappa\theta\sqrt{2\mathfrak{m}}b_1}{2}t^{5/4} + \mathcal{O}\left(t^{3/2}\right).\end{aligned}$$

Consequently,

$$\begin{aligned}
\frac{\widetilde{\Lambda}_t\left(u_t^* + \mathtt{i}ut^{1/2-\theta}\right) - \widetilde{\Lambda}_t\left(u_t^*\right)}{\sqrt{t}} &= \widetilde{\mathrm{C}}_1(u) - \widetilde{\mathrm{C}}_2 + \log \mathrm{M}_{\mathcal{V}}(\widetilde{\mathrm{D}}_1(u)) - \log \mathrm{M}_{\mathcal{V}}(\widetilde{\mathrm{D}}_2) \\
&= \frac{\gamma_0\left(\widetilde{\mathrm{D}}_1(u) - \widetilde{\mathrm{D}}_2\right)}{\left(\mathfrak{m} - \widetilde{\mathrm{D}}_1(u)\right)\left(\mathfrak{m} - \widetilde{\mathrm{D}}_2\right)} + \gamma_0\gamma_1\left(\log\left(\mathfrak{m} - \widetilde{\mathrm{D}}_1(u)\right) - \log\left(\mathfrak{m} - \widetilde{\mathrm{D}}_2\right)\right) + o(1) \\
&= \frac{\gamma_0\left(\mathtt{i}u\sqrt{2\mathfrak{m}}t^{1/2-\theta} + o(\sqrt{t})\right)}{2\mathfrak{m}b_1^2 t^{1/2}}\left[1 - \frac{\mathtt{i}ut^{1/4-\theta}}{b_1} + \mathcal{O}\left(t^{1/4}\right)\right] + \frac{\mathtt{i}u\gamma_0\gamma_1 t^{1/4-\theta}}{b_1} + o(1) \\
&= \frac{\mathtt{i}\gamma_0 u}{\sqrt{2\mathfrak{m}}b_1^2}t^{-\theta} + \frac{\gamma_0 u^2}{\sqrt{2\mathfrak{m}}b_1^3} + o(1),
\end{aligned}$$

and the proof follows by noticing that $b_1 < 0$ and $\gamma_0 = x\sqrt{2\mathfrak{m}}b_1^2$ from Lemma D.1. ∎

We finally prove the main theorem, when $x > 0$. The price of a European Call option with strike e^x is

$$\begin{aligned}
\mathbb{E}^{\mathbb{P}}\left(\mathrm{e}^{X_t} - \mathrm{e}^x\right)^+ &= \mathbb{E}^{\mathbb{Q}_t}\left[\left(\mathrm{e}^{X_t} - \mathrm{e}^x\right)^+ \frac{\mathrm{d}\mathbb{P}}{\mathrm{d}\mathbb{Q}_t}\right] = \mathbb{E}^{\mathbb{Q}_t}\left[\exp\left(\frac{-u_t^*(x)X_t + \widetilde{\Lambda}_t(u_t^*(x))}{t^{1/2}}\right)\left(\mathrm{e}^{X_t} - \mathrm{e}^x\right)^+\right] \\
&= \exp\left(\frac{-xu_t^*(x) + \widetilde{\Lambda}_t(u_t^*(x))}{\sqrt{t}}\right)\mathrm{e}^x\mathbb{E}^{\mathbb{Q}_t}\left[\exp\left(\frac{-u_t^*(x)(X_t - x)}{\sqrt{t}}\right)\left(\mathrm{e}^{X_t - x} - 1\right)^+\right] \\
&= \exp\left(\frac{-xu_t^*(x) + \widetilde{\Lambda}_t(u_t^*(x))}{\sqrt{t}}\right)\mathrm{e}^x\mathbb{E}^{\mathbb{Q}_t}\left[\exp\left(\frac{-u_t^*(x)Z_t}{\sqrt{t}/\vartheta(t)}\right)\left(\mathrm{e}^{Z_t\vartheta(t)} - 1\right)^+\right].
\end{aligned}$$

Case $\omega = 2$. The proof is identical to [39, Theorem 3.1] and is therefore omitted.

Case $\omega = 1$. The Fourier transform of the modified payoff $\exp\left(-\frac{u_t^*(x)Z_t}{\sqrt{t}}\right)\left(\mathrm{e}^{Z_t} - 1\right)^+$ under $\mathbb{Q}_t$ is

$$\begin{aligned}
\int_0^\infty \exp\left(-\frac{u_t^*(x)z}{\sqrt{t}}\right)\left(\mathrm{e}^z - 1\right)\mathrm{e}^{\mathtt{i}uz}\mathrm{d}z &= \left[\frac{\mathrm{e}^{(1+\mathtt{i}u-u_t^*(x)t^{-1/2})z}}{1 + \mathtt{i}u - u_t^*(x)t^{-1/2}}\right]_0^\infty - \left[\frac{\mathrm{e}^{(\mathtt{i}u-u_t^*(x)t^{-1/2})z}}{\mathtt{i}u - u_t^*(x)t^{-1/2}}\right]_0^\infty \\
&= \frac{1}{\mathtt{i}u - u_t^*(x)t^{-1/2}} - \frac{1}{1 + \mathtt{i}u - u_t^*(x)t^{-1/2}} \\
&= \frac{t}{\left(u_t^*(x) - (1 + \mathtt{i}u)\sqrt{t}\right)\left(u_t^*(x) - \mathtt{i}u\sqrt{t}\right)},
\end{aligned}$$

where in the second line we use the fact that $\lim_{t\downarrow 0} u_t^*(x)t^{-1/2} = +\infty$. Recall that the Gamma distribution with shape $|\gamma_0|$ and scale $|\frac{x}{\gamma_0}|$ has density $f_\Gamma \in L^2(\mathbb{R})$ given by

$$f_\Gamma(y) = \frac{y^{|\gamma_0|-1}}{\Gamma\left(|\gamma_0|\right)}\exp\left(-\left|\frac{\gamma_0}{x}\right|y\right)\left(\left|\frac{\gamma_0}{x}\right|\right)^{|\gamma_0|} \quad \text{for } y > 0. \tag{D.7}$$

Applying [35, Theorem 13.E] and Lemma D.3,

$$\mathbb{E}^{\mathbb{Q}_t}\left[\exp\left(\frac{-u_t^*(x)Z_t}{\sqrt{t}}\right)\left(\mathrm{e}^{Z_t}-1\right)^+\right] = \frac{t}{2\pi}\int_{-\infty}^{\infty}\frac{\Psi_t(u)\mathrm{d}u}{\left(u_t^*(x)-(1-\mathtt{i}u)\sqrt{t}\right)\left(u_t^*(x)+\mathtt{i}u\sqrt{t}\right)}$$

$$= \frac{t}{4\pi\mathfrak{m}}\int_{-\infty}^{\infty}\mathrm{e}^{-\mathtt{i}ux}\left(1-\frac{\mathtt{i}ux}{|\gamma_0|}\right)^{\gamma_0}(1+o(1))\,\mathrm{d}u = \frac{tf_\Gamma(x)}{2\mathfrak{m}}(1+o(1)), \tag{D.8}$$

where the last line follows from Fourier inversion. Combining Lemma D.2 and (D.8), the call price reads

$$\mathbb{E}\left(\mathrm{e}^{X_t}-\mathrm{e}^x\right)^+ = \exp\left(-\frac{\Lambda^*(x)}{\sqrt{t}}+x+c_2(x)+\gamma_1\right)\left(\frac{x}{|\gamma_0|\sqrt{2\mathfrak{m}}}\right)^{|\gamma_0|}\frac{f_\Gamma(x)}{2\mathfrak{m}}t^{1-\frac{|\gamma_0|}{2}}(1+o(1)) \quad \text{for } x>0.$$

Assuming now that $x<0$, the price of a European Put option with strike e^x is

$$\mathbb{E}\left(\mathrm{e}^x-\mathrm{e}^{X_t}\right)^+ = \exp\left(\frac{-xu_t^*(x)+\widetilde{\Lambda}_t(u_t^*(x))}{\sqrt{t}}\right)\mathrm{e}^x\mathbb{E}^{\mathbb{Q}_t}\left[\exp\left(\frac{-u_t^*(x)Z_t}{\sqrt{t}}\right)\left(1-\mathrm{e}^{Z_t}\right)^+\right],$$

and the Fourier transform of the modified payoff function $\exp\left(\frac{-u_t^*(x)Z_t}{\sqrt{t}}\right)\left(1-\mathrm{e}^{Z_t}\right)^+$ is

$$\int_{-\infty}^{0}\exp\left(-\frac{u_t^*(x)z}{\sqrt{t}}\right)(1-\mathrm{e}^z)\,\mathrm{e}^{\mathtt{i}uz}\mathrm{d}z = \frac{t}{\left(u_t^*(x)-(1+\mathtt{i}u)\sqrt{t}\right)\left(u_t^*(x)-\mathtt{i}u\sqrt{t}\right)}.$$

Following a similar procedure, and noticing that $(\mathrm{e}^{X_t})_{t\geq 0}$ is a $\mathbb{P}$-martingale, the put-call parity implies

$$\mathbb{E}\left(\mathrm{e}^{X_t}-\mathrm{e}^x\right)^+ = (1-\mathrm{e}^x)+\exp\left(-\frac{\Lambda^*(x)}{\sqrt{t}}+x+c_2(x)+\gamma_1\right)\left(\frac{|x|}{|\gamma_0|\sqrt{2\mathfrak{m}}}\right)^{|\gamma_0|}\frac{f_\Gamma(|x|)}{2\mathfrak{m}}t^{1-\frac{|\gamma_0|}{2}}(1+o(1))$$

for $x<0$.

In the standard Black–Scholes model with volatility $\Sigma>0$, the short-time asymptotics of the call option price reads [26, Corollary 3.5] $\mathbb{E}\left(\mathrm{e}^{X_t}-\mathrm{e}^x\right)^+ = (1-\mathrm{e}^x)^+ + \frac{1}{\sqrt{2\pi x^2}}\exp\left(-\frac{x^2}{2\Sigma^2 t}+\frac{x}{2}\right)(\Sigma^2 t)^{3/2}(1+\mathcal{O}(t))$. Then the asymptotics of implied volatility can be derived following the systematic approach provided in [32].

D.3. Proof of Theorem 4.16. We first prove the large deviations statement, which we then translate into the large-maturity behavior of the implied volatility. Andersen and Piterbarg [3, Proposition 3.1] analyzed moment explosions in the standard Heston model and proved that for any $u>1$ the quantity $\mathbb{E}(\mathrm{e}^{uX_t})$ always exists as long as

$$\kappa > \rho\xi u \qquad \text{and} \qquad d(u)\geq 0. \tag{D.9}$$

Moreover, the assumption $\kappa>\rho\xi$ implies (see [25]) that (D.9) holds for any $u\in[\overline{u}_-,\overline{u}_+]$, so that $\mathbb{E}(\mathrm{e}^{uX_t})$ is well defined for $u\in[\overline{u}_-,\overline{u}_+]$ and any (large) t in the standard Heston model. The tower property then yields

$$\mathrm{M}(t,u) = \mathbb{E}\left[\mathbb{E}(\mathrm{e}^{uX_t}|\mathcal{V})\right] = \mathrm{C}(t,u)\left(\mathrm{M}_{\mathcal{V}}\circ\mathrm{D}(t,u)\right).$$

Consequently, for any large t, $\mathrm{M}(t,u)$ is well defined for $u \in \mathcal{S} := [\overline{u}_-, \overline{u}_+] \cap \mathcal{S}_{\mathcal{V}}$, where the set $\mathcal{S}_{\mathcal{V}}$ is defined by

$$\mathcal{S}_{\mathcal{V}} := \bigcup_{t>0} \bigcap_{s \geq t} \{u : \mathrm{D}(s,u) < \mathfrak{m}\}.$$

Using the expressions of functions C and D in (A.1), the rescaled cgf of the process $(t^{-1}X_t)_{t\geq 0}$ reads

$$\begin{aligned}\Xi(t,u) &:= \frac{1}{t}\log\mathbb{E}\left(\mathrm{e}^{uX_t}\right) = \frac{1}{t}\mathrm{C}(t,u) + \frac{1}{t}\log \mathrm{M}_{\mathcal{V}}\left(\mathrm{D}(t,u)\right) \\ &= \frac{\kappa\theta(\kappa - \rho\xi u - d(u))}{\xi^2} - \frac{2\kappa\theta}{\xi^2 t}\log\left(\frac{1-g(u)\mathrm{e}^{-d(u)t}}{1-g(u)}\right) \\ &\quad + \frac{1}{t}\log \mathrm{M}_{\mathcal{V}}\left(\frac{\kappa - \rho\xi u - d(u)}{\xi^2}\frac{1-\mathrm{e}^{-d(u)t}}{1-g(u)\mathrm{e}^{-d(u)t}}\right).\end{aligned} \tag{D.10}$$

For any $u \in (\overline{u}_-, \overline{u}_+)$, since the quantity $d(u)$ is strictly positive, then

$$\lim_{t\uparrow\infty}\frac{1}{t}\log\left(\frac{1-g(u)\mathrm{e}^{-d(u)t}}{1-g(u)}\right) = 0 \quad \text{and} \quad \lim_{t\uparrow\infty}\frac{\kappa-\rho\xi u - d(u)}{\xi^2}\frac{1-\mathrm{e}^{-d(u)t}}{1-g(u)\mathrm{e}^{-d(u)t}} = \frac{\kappa-\rho\xi u-d(u)}{\xi^2}. \tag{D.11}$$

Since $u \mapsto \Xi(t,u)$ is continuous for each $t>0$, L'Hôpital's rule implies that $\lim_{t\uparrow\infty}\Xi(t,\overline{u}_\pm) = \kappa\theta(\kappa - \rho\xi\overline{u}_\pm)/\xi^2$.

Case $\mathfrak{m} = \infty$. Obviously $\mathcal{S}_{\mathcal{V}} = \mathbb{R}$, implying that $\mathcal{S} = [\overline{u}_-, \overline{u}_+]$. Equation (D.10) shows that

$$\Xi(u) := \lim_{t\uparrow\infty}\Xi(t,u) \equiv \mathfrak{L}(u) \quad \text{for any } u \in \mathbb{R},$$

with $\mathfrak{L}$ provided in (4.11). In [25, Theorem 2.1], it is proved that the limiting function Ξ and its effective domain $\mathcal{S}$ satisfy all the assumptions of the Gärtner–Ellis theorem (Theorem B.2), and hence the large deviations principle for the sequence $(t^{-1}X_t)_{t\geq 0}$ follows.

Case $\mathfrak{m} < \infty$. Equation (D.11) implies that

$$\left\{u : \frac{\kappa-\rho\xi u - d(u)}{\xi^2} < \mathfrak{m}\right\} \subset \mathcal{S}_{\mathcal{V}} \subset \left\{u : \frac{\kappa-\rho\xi u-d(u)}{\xi^2} \leq \mathfrak{m}\right\}.$$

As a result, the essential smoothness of function Ξ is guaranteed if

$$[\overline{u}_-, \overline{u}_+] \subset \left\{u : \frac{\kappa-\rho\xi u-d(u)}{\xi^2} < \mathfrak{m}\right\} = \left\{u : \kappa - \rho\xi u < \xi^2\mathfrak{m} + \sqrt{(\kappa-\rho\xi u)^2 + \xi^2 u(1-u)}\right\}.$$

Since $\kappa - \rho\xi u > 0$ holds for any $u \in [\overline{u}_-, \overline{u}_+]$,

$$\begin{aligned}\kappa-\rho\xi u < \xi^2\mathfrak{m} + \sqrt{(\kappa-\rho\xi u)^2+\xi^2u(1-u)} &\iff 0 < u(1-u) + \xi^2m^2 + 2\mathfrak{m}\sqrt{(\kappa-\rho\xi u)^2+\xi^2u(1-u)} \\ &\iff \frac{u(u-1)}{\xi^2} < \mathfrak{m}^2 + \frac{2\mathfrak{m}}{\xi^2}\sqrt{(\kappa-\rho\xi u)^2+\xi^2u(1-u)}.\end{aligned} \tag{D.12}$$

Since $[0,1] \subset (\overline{u}_-, \overline{u}_+)$, condition (D.12) holds for any $u \in [0,1]$. Whenever $u > 1$ or $u < 0$, as functions of u, the left-hand side is strictly increasing while the right-hand side is strictly decreasing. Therefore, (D.12) holds for any $u \in [\overline{u}_-, \overline{u}_+]$ if and only if $\max\{\overline{u}_-(\overline{u}_- - 1), \overline{u}_+(\overline{u}_+ - 1)\} < \mathfrak{m}^2\xi^2$. Consequently, Assumption 4.14 ensures that $\mathcal{S} = [\overline{u}_-, \overline{u}_+]$, and the proof follows from the Gärtner–Ellis theorem (Theorem B.2).

We now prove the asymptotic behavior for the implied volatility. We claim that in a randomized Heston setting the European option price has the following limiting behavior:

$$\begin{aligned}
-\lim_{t\uparrow\infty} \frac{1}{t} \log\left(\mathbb{E}\left(\mathrm{e}^{X_t} - \mathrm{e}^{xt}\right)^+\right) &= \mathfrak{L}^*(x) - x && \text{for } x \geq \frac{\overline{\theta}}{2}, \\
-\lim_{t\uparrow\infty} \frac{1}{t} \log\left(1 - \mathbb{E}\left(\mathrm{e}^{X_t} - \mathrm{e}^{xt}\right)^+\right) &= \mathfrak{L}^*(x) - x && \text{for } -\frac{\theta}{2} \leq x \leq \frac{\overline{\theta}}{2}, \\
-\lim_{t\uparrow\infty} \frac{1}{t} \log\left(\mathbb{E}\left(\mathrm{e}^{xt} - \mathrm{e}^{X_t}\right)^+\right) &= \mathfrak{L}^*(x) - x && \text{for } x \leq -\frac{\theta}{2}.
\end{aligned}$$

The proof is covered in detail in [40, section 5.2.2], and we therefore highlight the main ideas for completeness. From Theorem 4.16, define a time-dependent probability measure $\mathbb{Q}_t$:

$$\frac{\mathrm{d}\mathbb{Q}_t}{\mathrm{d}\mathbb{P}} := \exp\left\{u^*(x)X_t - \Xi\left(t, u^*(x)\right)t\right\},$$

where $u^*(x)$ is the solution to the equation $x = \Xi'(u)$. The option price is then expressed as the expectation under $\mathbb{Q}_t$ of a modified payoff and can be computed by (inverse) Fourier transform with the main contribution equal to $\exp\{-(\mathfrak{L}^*(x) - x)\,t\}$. It is also known (see [24, Corollary 2.12], for instance) that in the Black–Scholes model with volatility Σ the asymptotics of European option prices with strike e^{xt} are given by

$$\begin{aligned}
-\lim_{t\uparrow\infty} \frac{1}{t} \log\left(\mathbb{E}\left(\mathrm{e}^{X_t} - \mathrm{e}^{xt}\right)^+\right) &= \Lambda^*_{\mathrm{BS}}(x, \Sigma) - x && \text{for } x \geq \frac{\Sigma^2}{2}, \\
-\lim_{t\uparrow\infty} \frac{1}{t} \log\left(1 - \mathbb{E}\left(\mathrm{e}^{X_t} - \mathrm{e}^{xt}\right)^+\right) &= \Lambda^*_{\mathrm{BS}}(x, \Sigma) - x && \text{for } -\frac{\Sigma^2}{2} \leq x \leq \frac{\Sigma^2}{2}, \\
-\lim_{t\uparrow\infty} \frac{1}{t} \log\left(\mathbb{E}\left(\mathrm{e}^{xt} - \mathrm{e}^{X_t}\right)^+\right) &= \Lambda^*_{\mathrm{BS}}(x, \Sigma) - x && \text{for } x \leq -\frac{\Sigma^2}{2},
\end{aligned}$$

where $\Lambda^*_{\mathrm{BS}}(x, \Sigma) := \frac{\left(x + \Sigma^2/2\right)^2}{2\Sigma^2}$. Then the leading order of the large-time implied variance is obtained by solving

$$\mathfrak{L}^*(x) - x = \Lambda^*_{\mathrm{BS}}(x, \Sigma) - x = \frac{\left(-x + \Sigma^2/2\right)^2}{2\Sigma^2}.$$

We omit the details of the proof, which can be found in [25, 27].

REFERENCES

[1] H. Albrecher, P. Mayer, W. Schoutens, and J. Tistaert, *The little Heston trap*, Wilmott Magazine, January 2007, pp. 83–92.

[2] E. Alòs, J. A. León, and J. Vives, *On the short-time behavior of the implied volatility for jump-diffusion models with stochastic volatility*, Finance Stoch., 11 (2007), pp. 571–589.
[3] L. Andersen and V. Piterbarg, *Moment explosions in stochastic volatility models*, Finance Stoch., 11 (2007), pp. 29–50.
[4] L. Andersen, *Efficient Simulation of the Heston Stochastic Volatility Model*, preprint, http://ssrn.com/abstract=946405, 2007.
[5] G. Bakshi, C. Cao, and Z. Chen, *Empirical performance of alternative option pricing models*, J. Finance, 52 (1997), pp. 2003–2049.
[6] D. S. Bates, *Jumps and stochastic volatility: Exchange rate processes implicit in Deutsche Mark options*, Rev. Financ. Stud., 9 (1996), pp. 69–107.
[7] C. Bayer, P. Friz, and J. Gatheral, *Pricing under rough volatility*, Quant. Finance, 16 (2016), pp. 887–904.
[8] S. Benaim and P. Friz, *Smile asymptotics* 2: *Models with known moment generating function*, J. Appl. Probab., 45 (2008), pp. 16–32.
[9] S. Benaim and P. Friz, *Regular variation and smile asymptotics*, Math. Finance, 19 (2009), pp. 1–12.
[10] N. H. Bingham, C. M. Goldie, and J. L. Teugels, *Regular Variation*, Cambridge University Press, Cambridge, UK, 1989.
[11] D. Brigo, *The General Mixture-Diffusion SDE and Its Relationship with an Uncertain-Volatility Option Model with Volatility-Asset Decorrelation*, preprint, https://arxiv.org/abs/0812.4052, 2008.
[12] D. Brigo, F. Mercurio, and F. Rapisarda, *Lognormal-mixture dynamics and calibration to market volatility smiles*, Int. J. Theoret. Appl. Finance, 5 (2002), pp. 427–446.
[13] F. Caravenna and J. Corbetta, *General smile asymptotics with bounded maturity*, SIAM Financial Math., 7 (2016), pp. 720–759, https://doi.org/10.1137/15M1031102.
[14] P. Carr and D. B. Madan, *Option valuation using the fast Fourier transform*, J. Comput. Finance, 2 (1999), pp. 61–73.
[15] J. C. Cox, J. E. Ingersoll, and S. A. Ross, *A theory of the term structure of interest rates*, Econometrica, 53 (1985), pp. 385–407.
[16] H. Cramér, *Sur un nouveau théorème-limite de la théorie des probabilités*, Actualités Scientifiques Indust., 736 (1938), pp. 5–23.
[17] S. De Marco and C. Martini, *The term structure of implied volatility in symmetric models with applications to Heston*, Int. J. Theoret. Appl. Finance, 15 (2012), 1250026.
[18] A. Dembo and O. Zeitouni, *Large deviations via parameter dependent change of measure and an application to the lower tail of Gaussian processes*, in Seminar on Stochastic Analysis, Random Fields and Applications (Ascona, 1993), Progress Probab. 36, Birkhäuser, Basel, Switzerland, 1995, pp. 111–121.
[19] A. Dembo and O. Zeitouni, *Large Deviations Techniques and Applications*, Springer-Verlag, Berlin, Heidelberg, 1998.
[20] D. Dufresne, *The Integrated Square-Root Process*, Research Paper 90, University of Melbourne, Melbourne, Australia, 2001.
[21] O. El Euch and M. Rosenbaum, *Perfect hedging in rough Heston models*, Ann. Appl. Probab., 28 (2018), pp. 3813–3856.
[22] O. El Euch and M. Rosenbaum, *The characteristic function of rough Heston models*, Math. Finance, 29 (2019), pp. 3–38.
[23] O. El Euch, M. Fukasawa, and M. Rosenbaum, *The microstructural foundations of leverage effect and rough volatility*, Finance Stoch., 22 (2018), pp. 241–280.
[24] M. Forde and A. Jacquier, *Small-time asymptotics for implied volatility under the Heston model*, Int. J. Theor. Appl. Finance, 12 (2009), pp. 861–876.
[25] M. Forde and A. Jacquier, *The large-maturity smile for the Heston model*, Finance Stoch., 15 (2011), pp. 755–780.
[26] M. Forde, A. Jacquier, and R. Lee, *The small-time smile and term structure of implied volatility under the Heston model*, SIAM J. Financial Math., 3 (2012), pp. 690–708, https://doi.org/10.1137/110830241.
[27] M. Forde, A. Jacquier, and A. Mijatović, *Asymptotic formulae for implied volatility under the Heston model*, Proc. Roy. Soc. A, 466 (2010), pp. 3593–3620.

[28] M. Forde and H. Zhang, *Asymptotics for rough stochastic volatility models*, SIAM J. Financial Math., 8 (2017), pp. 114–145, https://doi.org/10.1137/15M1009330.
[29] J.-P. Fouque and B. Ren, *Approximation for option prices under uncertain volatility*, SIAM Financial Math., 5 (2014), pp. 360–383, https://doi.org/10.1137/130908385.
[30] P. Friz, S. Gerhold, and A. Pinter, *Option pricing in the moderate deviations regime*, Math. Finance, 28 (2018), pp. 962–988.
[31] M. Fukasawa, *Short-time at-the-money skew and rough fractional volatility*, Quant. Finance, 17 (2017), pp. 189–198.
[32] K. Gao and R. Lee, *Asymptotics of implied volatility to arbitrary order*, Finance Stoch., 18 (2014), pp. 342–392.
[33] J. Gatheral, *The Volatility Surface: A Practitioner's Guide*, Wiley, New York, 2006.
[34] J. Gatheral, T. Jaisson, and M. Rosenbaum, *Volatility is rough*, Quant. Finance, 18 (2018), pp. 933–949.
[35] R. Goldberg, *Fourier Transforms*, Cambridge University Press, Cambridge, UK, 1965.
[36] H. Guennoun, A. Jacquier, P. Roome, and F. Shi, *Asymptotic behavior of the fractional Heston model*, SIAM J. Financial Math., 9 (2018), pp. 1017–1045, https://doi.org/10.1137/17M1142892.
[37] S. L. Heston, *A closed-form solution for options with stochastic volatility with applications to bond and currency options*, Rev. Financ. Stud., 6 (1993), pp. 327–343.
[38] A. Jacquier, M. Keller-Ressel, and A. Mijatović, *Large deviations and stochastic volatility with jumps: asymptotic implied volatility for affine models*, Stochastics, 85 (2013), pp. 321–345.
[39] A. Jacquier and P. Roome, *The small-maturity Heston forward smile*, SIAM Financial Math., 4 (2013), pp. 831–856, https://doi.org/10.1137/13091703X.
[40] A. Jacquier and P. Roome, *Asymptotics of forward implied volatility*, SIAM Financial Math., 6 (2015), pp. 307–351, https://doi.org/10.1137/140960712.
[41] A. Jacquier and P. Roome, *Black-Scholes in a CEV random environment*, Math. Financial Economics, 12 (2018), pp. 445–474.
[42] A. Janick, T. Kluge, R. Weron, and U. Wystup, *FX smile in the Heston model*, in Statistical Tools for Finance and Insurance, Springer, Heidelberg, 2010, pp. 133–162.
[43] B. Jorgensen, *The Theory of Dispersion Models*, Chapman and Hall, London, 1997.
[44] I. Karatzas and S. E. Shreve, *Brownian Motion and Stochastic Calculus*, Springer, New York, 1991.
[45] R. Lee, *The moment formula for implied volatility at extreme strikes*, Math. Finance, 14 (2004), pp. 469–480.
[46] S. Mechkov, *"Hot-start" initialization of the Heston model*, Risk, 2016.
[47] A. Mijatović and P. Tankov, *A new look at short-term implied volatility in asset price models with jumps*, Math. Finance, 26 (2016), pp. 149–183.
[48] D. Revuz and M. Yor, *Continuous Martingales and Brownian Motion*, Springer, Berlin, 1999.
[49] P. Tankov, *Pricing and hedging in exponential Lévy models: Review of recent results*, in Paris-Princeton Lectures on Mathematical Finance, Springer, Berlin, 2010, pp. 319–359.
[50] D. Williams, *Probability with Martingales*, Cambridge University Press, Cambridge, UK, 1991.
[51] Zeliade Systems, *Heston* 2010, Zeliade Systems White Paper, http://www.zeliade.com/whitepapers/zwp-0004.pdf, 2011.